Summer 8-31-2016

Hamiltonian bifurcations in Schrodinger trimers

Casayndra H. Basarab
New Jersey Institute of Technology

Copyright Warning & Restrictions

The copyright law of the United States (Title 17, United States Code) governs the making of photocopies or other reproductions of copyrighted material.

Under certain conditions specified in the law, libraries and archives are authorized to furnish a photocopy or other reproduction. One of these specified conditions is that the photocopy or reproduction is not to be "used for any purpose other than private study, scholarship, or research." If a, user makes a request for, or later uses, a photocopy or reproduction for purposes in excess of "fair use" that user may be liable for copyright infringement,

This institution reserves the right to refuse to accept a copying order if, in its judgment, fulfillment of the order would involve violation of copyright law.

Please Note: The author retains the copyright while the New Jersey Institute of Technology reserves the right to distribute this thesis or dissertation

Printing note: If you do not wish to print this page, then select "Pages from: first page # to: last page #" on the print dialog screen

ABSTRACT

HAMILTONIAN BIFURCATIONS IN SCHRÖDINGER TRIMERS

by
Casayndra H Basarab

The phase space of the three-mode discrete NLS in the nonlinear regime with periodic boundary conditions is investigated by reducing the degree of freedom from three down to two. The families of standing waves are enumerated and normal forms are used to describe several families of relative periodic orbits whose topologies change due to Hamiltonian Hopf bifurcations and transcritical bifurcations. The Hamiltonian Hopf bifurcation occurs when eigenvalues on the imaginary axis collide and split and has two types: elliptic and hyperbolic. These two types arise in the DNLS problem, and the families of periodic orbits are discussed as a conserved quantity N is changed. The stability of each standing wave solution is discussed both numerically and analytically to describe how the dynamics change under perturbation of the parameter N.

HAMILTONIAN BIFURCATIONS IN SCHRÖDINGER TRIMERS

by
Casayndra H Basarab

A Dissertation
Submitted to the Faculty of
New Jersey Institute of Technology and
Rutgers, The State University of New Jersey – Newark
in Partial Fulfillment of the Requirements for the Degree of
Doctor of Philosophy in Mathematical Sciences

Department of Mathematical Sciences
Department of Mathematics and Computer Science, Rutgers-Newark

August 2016

APPROVAL PAGE

HAMILTONIAN BIFURCATIONS IN SCHRÖDINGER TRIMERS

Casayndra H Basarab

Dr. Roy Goodman, Dissertation Advisor — Date
Associate Professor of Mathematical Sciences, New Jersey Institute of Technology

---

Dr. Denis Blackmore, Committee Member — Date
Professor of Mathematical Sciences, New Jersey Institute of Technology

---

Dr. Richard Moore, Committee Member — Date
Associate Professor of Mathematical Sciences, New Jersey Institute of Technology

---

Dr. Casey Diekman, Committee Member — Date
Assistant Professor of Mathematics, New Jersey Institute of Technology

---

Dr. Marian Gidea, Committee Member — Date
Professor of Mathematics, Yeshiva University

BIOGRAPHICAL SKETCH

Author: Casayndra H Basarab

Degree: Doctor of Philosophy

Date: August 2016

Undergraduate and Graduate Education:

- Doctor of Philosophy in Mathematical Sciences,
  New Jersey Institute of Technology, Newark, NJ, 2016
- Bachelors of Science in Applied Mathematics,
  New Jersey Institute of Technology, Newark, NJ, 2011

Major: Applied Mathematics

Presentations and Publications:

Poster Presentation

"Hamiltonian Bifurcations in Schrödinger Trimers". *FACM*, New Jersey Institute of Technology, Newark, NJ, 2014

For my loving father John Basarab (1952-2012). Thank you for supporting all that I do. I have not only pursued this to better myself and my future, but to bring honor to you and our family name.

ACKNOWLEDGMENT

First and foremost, I would like to deeply thank my advisor Dr. Roy Goodman for helping me to improve my programming and mathematical skills. I can truly say I learned so much from him and because of him. I have achieved my dream of becoming a math professor soley because he has pushed me to better myself as a graduate student. We have worked well together over these past few years and I am very proud and honored that I can put his name on what we have created and will create together. I would like to thank Dr. Marian Gidea, Dr. Richard Moore, Dr. Casey Diekman, and Dr. Denis Blackmore for serving on my committee.

A huge thank you to NJIT for providing me with the Gary Thomas Fellowship. I would like to thank Lawrence (Tony) Howell for helping me to find scholarships and opportunities as an undergraduate. It is because of him that I had the will and ability to go further with my education. I'd also like to thank Dr. Denis Blackmore for being like a mentor to me. His kind words and reassurance were always appreciated, as was his insight into the problem I was working on. Lastly, I would like to thank my parents, as they are not only the reason I exist, but the reason I have always strived for more out of life. They always let my creativity fly free, they always let me be who I am without question even when they didn't understand, and because they instilled the importance of learning, I can finally call myself a "doctor".

TABLE OF CONTENTS

Chapter **Page**

TABLE OF CONTENTS
(Continued)

Chapter **Page**

LIST OF FIGURES

CHAPTER 1

INTRODUCTION

1.1 Motivation

The nonlinear Schrödinger equation (NLS) is a fundamental partial differential equation in mathematical physics. It arises in optical fibers and wave guide arrays, water waves, semiconductors and in Bose-Einstein condensates (BECs); a state a matter that can be acheived when a dilute gas of Bosons is cooled to temperatures very near absolute zero. We focus more on the physical application of waves propogating in a waveguide. There are two types of waveguides; one of which is made of a cylinder of two layers of glass, the inner layer with a higher refractive glass, stretched to the thickness of about a human hair and many kilometers long.

In the discrete nonlinear Schrödinger (DNLS) equation, the spatial derivative is replaced by its finite difference approximation. It can model an array of optical wave guides, in which the light in each waveguide interacts with its immediate neighbors (by the time it gets to two neighbors away, the wave dissipates so much that its contribution is negligible). The DNLS was derived by Holstein as a model of molecular crystals [8].

We are interested in the dynamics of the three-mode DNLS in the weakly nonlinear regime, i.e., for small amplitudes. This allows for perturbation methods. Other studies have focused on the large amplitude regime, where the nonlinear part is dominant [33], while still others have revealed pitchfork bifurcations when studying

the two waveguide NLS [13]. The three mode DNLS trimer, the one we consider, is the simplest case in which Hamiltonian Hopf (HH) bifurcations arise, as they may occur in the NLS PDE with a spatial potential. This dissertation is a natural continuation of a paper by Goodman who studies the dynamics of the standing wave solutions of the nonlinear Schrödinger/GrossPitaevskii (NLS/GP) equation by constructing localized potentials [12].

Johansson studies the DNLS with three modes and periodic boundary conditions and focuses on the dipole mode which undergoes a Hamiltonian-Hopf bifurcation [19]. He describes the Hamiltonian Hopf bifurcation. He uses numerical continuation techniques to calculate solutions and finds the two different types of the Hamiltonian Hopf bifurcation. The main objective of this dissertation is to analytically calculate the standing wave solutions, find which solution undergoes the HH bifurcation and continue Johansson's work. We provide both analytical and numerical insight into the dynamics of these solutions and discuss how dynamics change when a parameter is varied so that we may better understand the structure of these bifurcations. We wish to further understand the two types of the Hamiltonian Hopf bifurcation analytically, making Johansson's paper the main motivator of this dissertation.

In addition to the analytical and numerical study of the trimer, experimental observations have been made for a three-well potential with a saturable nonlinearity. Kapitula et al. make an important numerical and analytical stability study of standing wave solutions to the NLS with a three-well potential and saturable nonlinearity in [20]. They find that "any state with multiple in-phase pulses is always unstable" and that one of the nonlinear normal mode (NNM) solutions undergoes

the HH bifurcation. Law and Hoq discuss the instability and evolution of stationary solutions to the focusing and defocusing cubic DNLS in one, two, and three spatial dimensions and summarize their own previous work and that of others [24].

A nonlinear normal mode of a Hamiltonian system is a family of periodic solutions that approaches, in the limit of small amplitude, a normal mode of the linearized system. These families of solutions have been widely studied in the past. Hennig, for example, proves the existence of NNMs for general systems of two coupled nonlinear oscillators leading to a comparison principle for ODEs, showing when the amplitude of NNMs goes to zero the linear normal modes (LNMs) are recovered [15]. Montaldi et al. [32] developed rigorous analytic methods for calculating NNMs. In a follow up paper, they show how to compute the spectral stability of said NNMs. Chechin and Sakhnenko introduced the idea of "bushes", families of normal modes belonging to subgroups of a system's symmetries [4]. Hennig et al. [16] study the idea of "discrete breathers" which arise from the nonlinearity and discrete parts of the system. They have an application to describing the motion of waves in arrays of nonlinear optical waveguides that can even be extended to biophysics or biomolecular engineering.

In addition to the above, many have been concerned with the symmetry and symmetry breaking of Hamiltonian systems, as this can force certain types of behavior. In particular, the symmetry of Hamiltonian systems can be used as a reduction [5]. We will see this in our problem later in Chapter 5. Symmetry reduction methods can be used to map a coupled system of four elements to a three-degree of freedom Hamiltonian system in reduced phase space [17]. Golubitsky has dedicated most of

his career to studying symmetry in ODEs. In one paper, he studies the bifurcations of equilibrium points in a one degree of freedom Hamiltonian system with symmetry leading to a theorem describing the action of a symmetry group on the zero eigenspace. Shlizerman et al. [22] find conditions for a symmetry-breaking bifurcation as a parameter N is changed in an NLS/GP equation with a two-well potential. This is actually the same parameter that we vary for our problem.

The first step in understanding the global phase space is to look at each simple solution of the DNLS. Stability analysis is used to check for bifurcations, and what kinds of families of solutions arise when modes become unstable. The HH bifurcation is characterized by a double zero of deficiency one on the imaginary axis, and happens when two pairs of purely imaginary eigenvalues collide on the imaginary axis and become a quartet as a control parameter is varied; see Figure 1.1. It is a fundamental mechanism that can give rise to the instability of nonlinear waves. We would further like to understand what types of orbits exist in a neighborhood of the Hamiltonian-Hopf bifurcation and therefore, need nonlinear analysis.

1.2 Set Up

The cubic DNLS is:

$$i\dot{\Psi}_j + \Psi_{j+1} - 2\Psi_j + \Psi_{j-1} + |\Psi_j|^2\Psi_j = 0. \tag{1.1}$$

It is the equation of motion for the Hamiltonian

$$H(i\mathbf{\Psi}, \bar{\mathbf{\Psi}}) = \sum_{j=1}^{\mathrm{n_{sites}}} (|\Psi_{j+1} - \Psi_j|^2 - \frac{1}{2}|\Psi_j|^4), \tag{1.2}$$

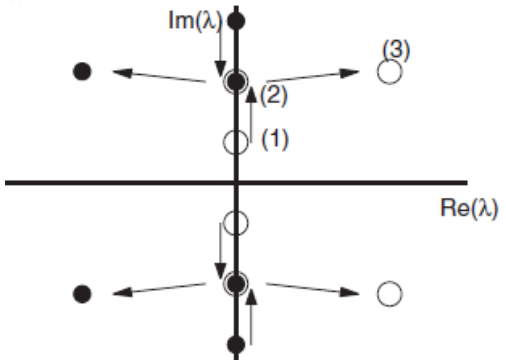

Figure 1.1 Eigenvalues collide along the imaginary axis and split off into a quartet as a parameter is varied.

where time t actually represents the distance down the waveguide. This equation is sometimes called the discrete self trapping (DST) and is referred to as a *focusing* DNLS because the derivative term $D\Psi = \Psi_{j+1} - 2\Psi_j + \Psi_{j-1}$ has the same sign as the nonlinear part $|\Psi_j|^2\Psi_j$. If the sign of the derivative term is changed, i.e., the DNLS is *defocusing*, the same standing wave solutions would arise, though the dynamics associated with them would be different. For the defocusing case, the dynamics for the nodal solution, i.e., the Hamiltonian Hopf bifurcation and its types would actually remain the same, however the dynamics would change for the other two standing wave solutions. In the PDE, the focusing can lead to a wave which is zero in width but infinite in height over a finite time, but there is no such thing that exists for the system of ODEs, since there is a restriction on height. The dynamics in the DNLS correspond to three-mode localized potentials in the continuous case, wherein the partial derivative not replaced by its finite difference, and is studied by Goodman [12].

We consider the special case of the DNLS trimer with three sites, or $n_{\text{sites}} = 3$ and periodic boundary conditions $\Psi_{j+3} = \Psi_j$ for $j = 0, 1$. We consider periodic boundary conditions because these give rise to the vortex solution, the standing wave solution of the form in Equation (3.3). If we were to consider say Dirichlet conditions, this would give only real valued standing waves, and no "moving solutions". It is found that

$$N = |\Psi_1|^2 + |\Psi_2|^2 + |\Psi_3|^2 \tag{1.3}$$

is a conserved quantity as a consequence of Nöther's Theorem, which states that there is a conserved quantity associated with each continuous symmetry. This system has the rotational symmetry $H(i\Psi_j, \bar{\Psi}_j) = H(ie^{i\Phi}\Psi_j, e^{-i\Phi}\bar{\Psi}_j)$. This parameter N can be thought of as a sort of "norm" and represents the brightness of light in a waveguide.

We can use Quantity (1.3) to reduce the number of the degrees of freedom from three down to two. There is a trade off to performing a reduction, however. While there are fewer variables and the problem is now in $\mathbb{R}^4$ rather than $\mathbb{R}^6$, the equations appear to be more complicated because there are new terms introduced and the problem loses some of the original symmetry.

A standing wave (relative fixed point) is a solution of the form

$$\mathbf{\Psi} = \begin{pmatrix} \Psi_1(N) \\ \Psi_2(N) \\ \Psi_3(N) \end{pmatrix} e^{-i\Omega(N)t}. \tag{1.4}$$

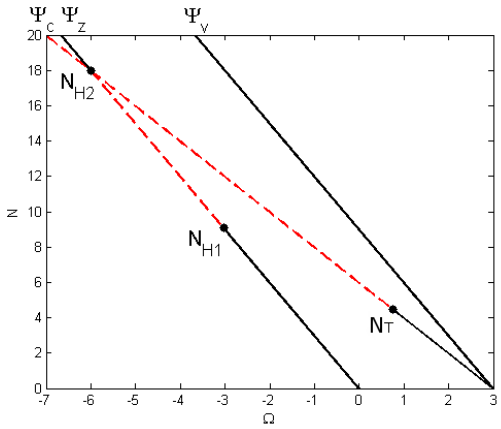

Figure 1.2 A power diagram of the relative fixed points of Solution (1.4). Solid lines indicate stability, while dashed lines indicate instability. The figure shows a transcritical bifurcation for solution Ψ_c at $N = N_T$, and two Hamiltonian Hopf bifurcations for Ψ_z at $N = N_{H_1}$ and $N = N_{H_2}$.

In Figure 1.2, plots of the three different types of solutions can be seen along with regions of the bifurcations that arise. We explain this in more detail later once there is an understanding of some key concepts.

In addition to these two real and one complex analytical solutions, Eilbeck et al. finds there are three more real analytical solutions to this problem, which are in parametric form [8]. In particular, the vectors associated with these solutions are of the form $(+,.,.)^\top$, $(+,+,.)^\top$ and $(-,+,+)^\top$. We do not study these three solutions but the reader should be made aware of their existence. These solutions do not undergo bifurcation. The first two solutions are branches which intersect with our $(+,+,+)$, what we call the constant solution, Equation (3.2) in Chapter 3. Eilbeck also mentions what happens in the presence of a large number of sites. For $n_{\text{sites}} = 100$ he discusses the stationary solutions for the self-trapping on crystalline acetanilide.

As the number of sites tend to infinity, this does not affect the standing wave solutions and dynamics for $n_{sites} = 3$. This is because we are looking far enough away where the discretization of the spatial derivative does not affect the full results of what is happening in the PDE.

1.3 Previous Research

Susanto summarizes previous research on the DNLS [35]. Clearly, the DNLS in Equation (1.1) is integrable for $n_{sites} = 1$. References [1] and [25] show that the dimer case ($n_{sites} = 2$) of the DNLS in (1.1) is integrable because the degrees of freedom is equal to the number of independent conserved quantities. However, the $n_{sites} \geq 3$ system is not integrable as evidenced by the chaotic dynamics seen by Johansson [19].

Sacchetti studied the generic n-well potential for the Schrödinger equation and the $n_{sites} = 4$ particle case in detail [34]. We choose to study the $n_{sites} = 3$ case because we are mostly interested in the HH bifurcation and the $n_{sites} = 3$ case is the simplest case where the HH bifurcation arises.

Hennig [14] uses algebraic methods to construct generalizations of the three-mode NLS that are completely integrable. Hennig [18] also indicates that the trimer may be chaotic by introducing a small parameter that couples the third oscillator to the integrable dimer system and then using Melnikov perturbation theory. Our aim is to study this system without such an artificial parameter. Buonsante also studies the fixed points and their stability of the chaotic solutions of the trimer as three coupled Bose-Einstein condensates [2].

A hallmark of non-integrable systems is the presence of chaos, as was seen by Eilbeck et al. [8]. The chaos was proven numerically by calculating the Lyapunov exponent [6]. Additional numerics were performed to show transitions between quasi-periodic behavior and chaos for the DST equations [9]. In 1992, Molina et al. [31] performed numerics on the $n_{sites} = 3$ case where two oscillators are nonlinear and the third is modified to be linear [30] [29].

The DNLS presents a set of coupled nonlinear classical oscillators introduced by Hennig as a model to describe the nonlinear vibrational dynamics in small polyatomic aggregates [17]. It has been a widely studied equation since the 1980s. Eilbeck and Johansson both worked on the problem and review the work that had been studied from the 1980's to the early 2000s in a paper titled "The Discrete Nonlinear Schrödinger Equation 20 Years On" [7].

1.4 Discussion of Outline

This dissertation is organized as follows. In Chapter 2, we discuss Hamiltonian systems, the HH bifurcation, Lyapunov families, normal forms, and other background knowledge needed to understand our many calculations. In Chapter 3 we discuss the form of the standing wave solutions, linearization and reduction of the number of the degrees of freedom. We then discuss the bifurcations that arise for each of these solutions. In Chapter 4 we compute the phase plane and Poincaré maps associated with the solution that undergoes the HH bifurcation. Chapter 5 shows more detail concerning the periodic orbits which undergoes the transcritical bifurcation. We

discuss future and current work in Chapter 6. Finally, we follow up with our concluding remarks in Chapter 7.

CHAPTER 2

HAMILTONIAN SYSTEMS

Before we can answer the questions posed above, we must understand Hamiltonian systems, normal forms, and the Hamiltonian Hopf bifurcation itself.

2.1 Hamiltonian Systems and the Poisson Bracket

We consider a general Hamiltonian system in n degrees of freedom. The evolution of the positions q and momenta p in $\mathbb{R}^n$ is given by $H(\mathbf{q}, \mathbf{p}, t)$ and system of ODEs

$$\begin{aligned} \dot{\mathbf{q}} &= \frac{\partial H}{\partial \mathbf{p}}, \\ \dot{\mathbf{p}} &= -\frac{\partial H}{\partial \mathbf{q}}, \end{aligned} \tag{2.1}$$

where $H(\mathbf{q}, \mathbf{p}, t)$ is a differentiable function.

The canonical Poisson bracket of two functions f and g is defined as

$$\{f, g\} = \frac{\partial f}{\partial \mathbf{p}}\frac{\partial g}{\partial \mathbf{q}} - \frac{\partial f}{\partial \mathbf{q}}\frac{\partial g}{\partial \mathbf{p}} = \sum_{i=1}^{n}\left(\frac{\partial f}{\partial p_i}\frac{\partial g}{\partial q_i} - \frac{\partial f}{\partial q_i}\frac{\partial g}{\partial p_i}\right).$$

This leads to the result that any function $f(\mathbf{p}(t), \mathbf{q}(t))$ has time derivative:

$$\begin{aligned} \frac{df}{dt} &= \frac{\partial f}{\partial \mathbf{p}}\dot{p} + \frac{\partial f}{\partial \mathbf{q}}\dot{q} + \frac{\partial f}{\partial t} \\ &= \sum_{i=1}^{n}\left(\frac{\partial f}{\partial p_i}\frac{\partial H}{\partial q_i} - \frac{\partial f}{\partial q_i}\frac{\partial H}{\partial p_i}\right) + \frac{\partial f}{\partial t} \\ &= \{f, H\} + \frac{\partial f}{\partial t}. \end{aligned}$$

Note if $\frac{\partial f}{\partial t} = 0$, then $\frac{df}{dt} = \{f, H\}$.

Given the Hamiltonian H, the position vector

$$\mathbf{x} = \begin{pmatrix} \mathbf{q} \\ \mathbf{p} \end{pmatrix} \tag{2.2}$$

and the symplectic matrix

$$J = \begin{pmatrix} 0 & I \\ -I & 0 \end{pmatrix}, \tag{2.3}$$

we can rewite the system of ODEs (2.1) using the Hamiltonian as follows:

$$\dot{\mathbf{x}} = J\nabla H. \tag{2.4}$$

2.2 Spectrum of Linear Hamiltonian Systems

In linear Hamiltonian systems, the configuration of the spectrum is constrained. If λ is an eigenvalue, then so are $-\lambda$, $\bar{\lambda}$, and $-\bar{\lambda}$. The only four possiblities are two purely real eigenvalues of opposite sign, two purely imaginary eigenvalues of opposite sign, the zero eigenvalue, and a "Krein quartet" when λ is of the form $\pm a \pm bi$, as is illustrated in Figure 2.1.

MacKay explains that depending on what type of eigenvalues there are in a system, different unfolding and stability changes occur [26]. The "Krein signature" of an eigenvalue measures whether the energy of a system is positive or negative. If λ

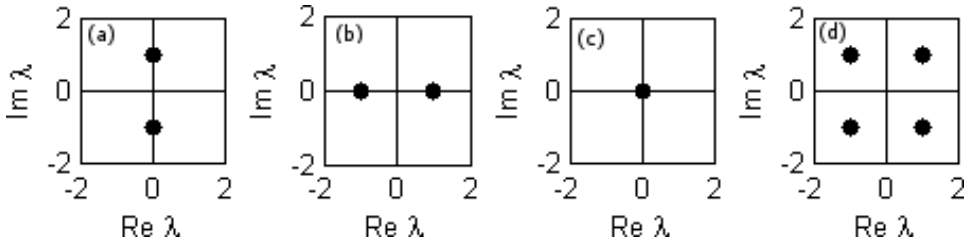

Figure 2.1 The spectrum of eigenvalues for a linear Hamiltonian system. a) λ imaginary, b) λ real, c) $\lambda = 0$, and d) λ is of the form $\pm a \pm bi$.

is a non zero pure imaginary simple eigenvalue, then the energy on the real invariant subspace is either positive or negative. The sign cannot change with continuous change of the Hamiltonian. In other words: start positive, stay positive. Start negative, stay negative. If two of these eigenvalues with the same sign of energy collide, then loss of linear stability cannot result. This idea comes from energy conservation. Further, stability can only be lost if two such eigenvalues of opposite signs of energy collide, or if there is a collision at the origin.

MacKay describes five different cases that show what happens when unfolding double eigenvalues on the imaginary axis as a smooth pair of equilibria is followed as parameters are varied. This can help one understand what will happen to a problem as parameters are varied, knowing of course, the codimension of the Jordan normal form, and whether it is diagonal.

Kapitula et al. considers purely imaginary eigenvalues and negative Krein signature for a Hamiltonian eigenvalue problem [21]. They can become unstable upon collision with other purely imaginary eigenvalues with positive signature. This yields the very thing we are concerned about: the HH bifurcation. The Krein matrix,

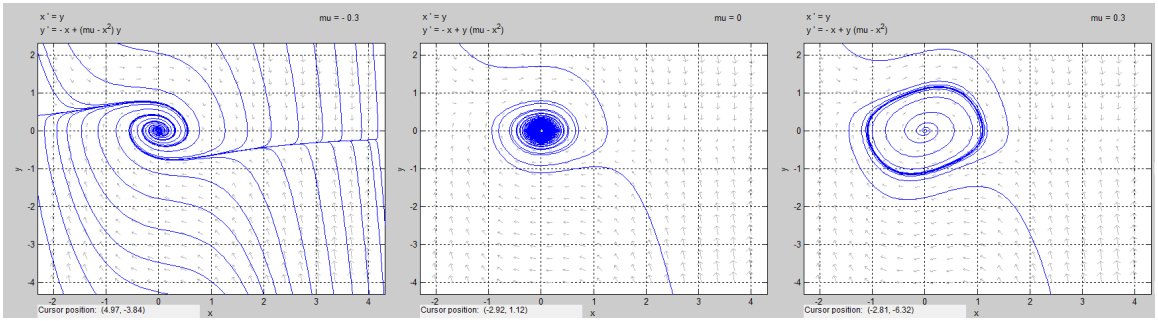

Figure 2.2 An example of the evolution of μ of the supercritical Hopf bifurcation for the Liénard equation.

computed numerically by Kapitula, can locate unstable eigenvalues and/or ones with negative Krein signature. These are zeros of the determinant.

2.3 Hamiltonian Hopf Bifurcation

The standard Hopf bifurcation occurs when a fixed point goes from stable to unstable (or vice versa) with a pair of eigenvalues crossing the imaginary axis as some parameter is changed. The supercritical case occurs when an unstable point is surrounded by a stable limit cycle, while the subcritical case occurs when a stable fixed point is surrounded by an unstable limit cycle. See Figure 2.2 for the evolution of a supercritical Hopf bifurcation for μ passing though zero, occurring in the Liénard equation.

The Hamiltonian Hopf bifurcation occurs when two pairs of eigenvalues starting on the imaginary axis collide and split off into a quartet, as can be seen in Figure 1.1. Further, there are two types of Hamiltonian Hopf bifurcation: the hyperbolic and elliptical cases in Figures 2.3a and 2.3b, respectively. These two plots describe

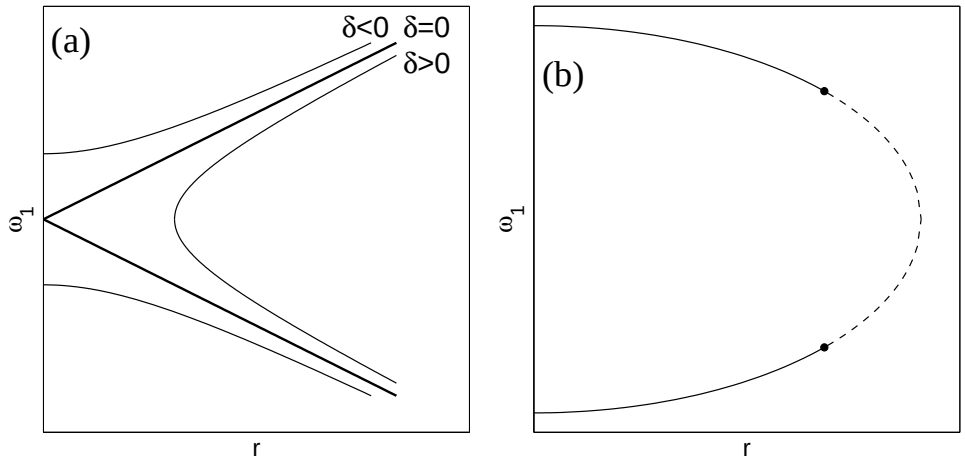

Figure 2.3 The hyperbolic (a) and elliptic (b) case of a Hamiltonian Hopf Bifurcation.

topological arrangements of periodic orbits in a neighborhood of the bifurcation and relate the amplitude r to the frequency ω of said orbits in a neighborhood of the bifurcation as a parameter N (which we explain later) changes through its critical values.

The two types of HH bifurcations can be determined by examining a particular quadratic form, coming from the coefficients of a normal form as in Subsection 3.3.3. Our analysis later in Subsection 3.3.3 illustrates the two HH bifurcations and explains what happens to these solutions as N in equation (1.3) passes through its critical values.

2.4 Lyapunov Families

The Lyapunov Center Theorem allows us to understand the existence of families of periodic solutions based on pairs of eigenvalues. Solutions which are families

of periodic solutions having zero amplitude are called "Lyapunov families" and are associated with the HH bifurcation. These families are the continuation of the linear oscillating solutions.

Lyapunov Center Theorem. *Assume that a system with a nondegenerate integral has equilibrium points with exponents* $\pm i\omega, \lambda_3, ..., \lambda_m$*, where* $i\omega \neq 0$ *is pure imaginary. If* $\lambda_j/i\omega$ *is never an integer for* $j = 3, ..., m$*, then there exists a one-parameter family of periodic orbits emanating from the equilibrium point. Moreover, when approaching the equilibrium point along the family, the periods tend to* $2\pi/\omega$ *and the nontrivial multipliers tend to* $exp\,(2\pi\lambda_j/\omega)$*,* $j = 3, ..., m$*. [27]*

That is, consider a Hamiltonian system $\dot{\mathbf{x}} = L\mathbf{x} + M(\mathbf{x})$ with $M(x) = O(|x|^2)$ the nonlinear part, and nonresonant eigenvalues $\pm i\omega_1, \pm i\omega_2, ...$ For each pair of eigenvalues, there is a family of periodic orbits emanating out of the origin existing in the linear problem that also exist in the nonlinear problem as long as there are no resonances.

The hyperbolic case of the HH bifurcation has two separate Lyapunov families. As a parameter N is varied, these two meet at the origin, and as N is varied further, they become a single family that disconnects from the origin. In the elliptic case, the two local families are joined into a single global branch that shrinks to a point and vanishes as the critical value of N is crossed. This can be seen in Figure 2.3 and was studied numerically or by series expansion in the 1960's by many including Deprit, Pedersen and Palmore, but later understood analytically by Meyer and Schmidt [28].

2.5 Normal Forms and Canonical Changes of Variables

Linearization and perturbation methods are used to simplify difficult problems in nonlinear dynamics. One such way of simplifying a Hamiltonian is a "normal form".

Given a Hamiltonian

$$H = \sum_{j=0}^{\infty} \delta^j H_j, \tag{2.5}$$

we can use a special near-identity symplectic change of variables called a "Lie Transform" to transform the Hamiltonian H into a form

$$H_{new} = \sum_{j=0}^{\infty} \delta^j K_j \tag{2.6}$$

so that the K_j are "simpler", at least to a certain order. This canonical change of variables preserves the structure of the Hamiltonian. In constructing this transformation however, additional terms of higher order are introduced.

In the neighborhood of a fixed point, H_0 is a quadratic form represented by a symmetric matrix, also called H_0. The dynamics due to the matrix H_0 are simply

$$\dot{\mathbf{x}} = JH_0\mathbf{x}.$$

Before the normal form (2.6) of the Hamiltonian (2.5) is computed, the matrix H_0 is generally put into its own normal form by the change of variables

$$\mathbf{x} = P\boldsymbol{\xi} \tag{2.7}$$

where P is a symplectic matrix (one that satisfies the condition $P^\top JP = J$) and

$$\xi = \begin{pmatrix} \xi_1 \\ \xi_2 \\ \eta_1 \\ \eta_2 \end{pmatrix}. \tag{2.8}$$

We then have that the change from $\mathbf{x}$ to $\boldsymbol{\xi}$ is

$$\begin{aligned} \dot{\mathbf{x}} &= JH_0\mathbf{x} \\ P\dot{\boldsymbol{\xi}} &= JH_0P\boldsymbol{\xi} \\ \dot{\boldsymbol{\xi}} &= P^{-1}JH_0P\boldsymbol{\xi} \\ \dot{\boldsymbol{\xi}} &= JP^{-1}H_0P\boldsymbol{\xi} \\ \dot{\boldsymbol{\xi}} &= JK_0\boldsymbol{\xi} \end{aligned}$$

where J is as in (2.3) and $K_0 = P^{-1}H_0P$.

The form for H for the HH bifurcation can be written as

$$H = H_2 + \delta\hat{H}_2 + \sum_{k=3}^{\infty} H_k, \tag{2.9}$$

where H_2 is the quadratic part, δ measures perturbation, $\hat{H}_2$ is the quadratic part of H that depends on δ and H_k are higher order terms of the Hamiltonian. Note that if $\mathbf{x}$ is of order $O(\sqrt{\delta})$, then $H_2 = O(\delta)$ and both $\delta\hat{H}_2$ and H_4 are $O(\delta^2)$. Dividing by δ

gives the general form for matrix

$$JK_0 = \left(\begin{array}{cc|cc} 0 & \Omega & 0 & 0 \\ -\Omega & 0 & 0 & 0 \\ \hline -\sigma & 0 & 0 & \Omega \\ 0 & -\sigma & -\Omega & 0 \end{array}\right). \tag{2.10}$$

The Burgoyne-Cushman algorithm computes a normal form for a real linear Hamiltonian with purely imaginary eigenvalues [3]. This algorithm is explained in more detail in the Appendix. It finds a canonical change of variables represented by a matrix P that simplifies H_2 in a neighborhood of an HH bifurcation. This algorithm is needed in order to quote a result later by Meyer and Hall [27] but it introduces more terms for $\hat{H}_2$ and H_4. While no change of variables exist that will eliminate $\hat{H}_2$ or H_4, the normal form (and a projection) computed later in Subsection 3.3.3 allows us to split $\hat{H}_2$ and H_4 into resonant and nonresonant terms. Nonresonant terms are removed at the expense of adding higher-order terms. For long but finite times, these can be ignored. Resonant terms are the ones that cannot be eliminated by the normalization procedure.

CHAPTER 3

LINEARIZING THE DNLS AND ANALYSIS OF SOLUTIONS

The three mode DNLS in Equation (1.1) can be rewritten as:

$$i\dot{\mathbf{\Psi}} = A\mathbf{\Psi} + N(\mathbf{\Psi}) \tag{3.1}$$

where

$$\mathbf{\Psi} = \begin{pmatrix} \Psi_1 \\ \Psi_2 \\ \Psi_3 \end{pmatrix},$$

$$A = \begin{pmatrix} -2 & 1 & 1 \\ 1 & -2 & 1 \\ 1 & 1 & -2 \end{pmatrix}$$

is the linear part of the DNLS, and

$$N(\mathbf{\Psi}) = \begin{pmatrix} |\Psi_1|^2\Psi_1 \\ |\Psi_2|^2\Psi_2 \\ |\Psi_3|^2\Psi_3 \end{pmatrix}$$

is the nonlinear part. This corresponds to the Hamiltonian (1.2) with

$$\mathbf{q} = i\mathbf{\Psi},$$

$$\mathbf{p} = \bar{\mathbf{\Psi}}.$$

3.1 Elementary Solutions

Equation (3.1) can be simplified by first diagonalizing the linear part of H by $\mathbf{\Psi}^\top A\mathbf{\Psi}$. The eigenvalues are $\lambda_1 = 0$ and $\lambda_2 = \lambda_3 = -3$ with associated normalized eigenvectors:

$$\mathbf{v}_1 = \frac{1}{\sqrt{3}}\begin{pmatrix}1\\1\\1\end{pmatrix},\ \mathbf{v}_2 = \frac{1}{\sqrt{2}}\begin{pmatrix}-1\\0\\1\end{pmatrix},\ \mathbf{v}_3 = \frac{1}{\sqrt{6}}\begin{pmatrix}1\\-2\\1\end{pmatrix}.$$

We define an orthogonal matrix M whose rows are the eigenvectors of A.

$$M = \begin{pmatrix} \frac{1}{\sqrt{3}} & \frac{1}{\sqrt{3}} & \frac{1}{\sqrt{3}} \\ -\frac{1}{\sqrt{2}} & 0 & \frac{1}{\sqrt{2}} \\ -\frac{1}{\sqrt{6}} & \frac{2}{\sqrt{6}} & -\frac{1}{\sqrt{6}} \end{pmatrix}$$

Hamilton's equations still apply for the canonical change of variables $(\mathbf{\Psi}, \bar{\mathbf{\Psi}}) = (M\mathbf{y}, M\bar{\mathbf{y}})$ and the new Hamiltonian is

$$\begin{aligned} H = 3|y_2|^2 + 3|y_3|^2 - \frac{1}{3}|y_1|^2|y_2|^2 - \frac{1}{6}|y_2|^2|y_3|^2 - \frac{1}{3}|y_1|^2|y_3|^2 \\ -\frac{1}{6}\left(y_1\bar{y}_2 + y_2\bar{y}_1\right)^2 - \frac{1}{12}\left(y_3\bar{y}_2 + y_3\bar{y}_2\right)^2 - \frac{1}{6}\left(y_1\bar{y}_3 + y_3\bar{y}_1\right)^2 \\ +\frac{1}{3\sqrt{2}}\left(y_1\bar{y}_2^2 y_3 + \bar{y}_1 {y_2}^2 \bar{y}_3\right) + \left(\frac{\sqrt{2}}{3}|y_2|^2 - \frac{1}{3\sqrt{2}}|y_3|^2\right)\left(\bar{y}_1 y_3 + y_1\bar{y}_3\right) \\ -\frac{1}{6}|y_1|^4 - \frac{1}{4}|y_2|^4 - \frac{1}{6}|y_3|^4 \end{aligned}$$

The system (3.1) has three different forms of nonlinear normal modes (NNMs), which are continuations of linear eigenvectors.

The three solutions depend on the conserved parameter N and are the constant solution

$$\mathbf{\Psi}_{\mathrm{c}} = \sqrt{\frac{N}{3}} \begin{pmatrix} 1 \\ 1 \\ 1 \end{pmatrix} e^{-i\frac{N}{3}t} = \sqrt{N}\mathbf{v}_1 e^{-i\frac{N}{3}t}, \tag{3.2}$$

the vortex solution

$$\mathbf{\Psi}_{\mathrm{v}} = \sqrt{\frac{N}{3}} \begin{pmatrix} e^{2\pi i/3} \\ 1 \\ e^{-2\pi i/3} \end{pmatrix} e^{i\left(3-\frac{N}{3}\right)t} = -\sqrt{\frac{N}{2}} \left(i\mathbf{v}_2 + \mathbf{v}_3\right) e^{i\left(3-\frac{N}{3}\right)t}, \tag{3.3}$$

and the nodal solution

$$\mathbf{\Psi}_{\mathrm{z}} = \sqrt{\frac{N}{2}} \begin{pmatrix} 1 \\ 0 \\ -1 \end{pmatrix} e^{i\left(3-\frac{N}{2}\right)t} = -\sqrt{N}\mathbf{v}_2 e^{i\left(3-\frac{N}{2}\right)t}. \tag{3.4}$$

Each of the three solutions are linear combinations of eigenvectors and are points about at which we linearize in the reduced system to learn of the dynamics of nearby orbits. It is important to note that in addition, the vector in the third solution (3.4) can be replaced by $(0, 1, -1)^\top$ or $(1, -1, 0)^\top$.

3.2 Reduction of the Degrees of Freedom

The first canonical change of variables is to action-angle variables

$$y_j = e^{i\theta_j}\sqrt{J_j},$$

for $j = 1, 2, 3$.

The second change allows for a reduction from three degrees of freedom to two.

$$\begin{aligned} J_1 &= \rho_1 \qquad J_2 = \rho_2 - \rho_1 - \rho_3 \qquad J_3 = \rho_3 \\ \theta_1 &= \phi_1 + \phi_2 \qquad \theta_2 = \phi_2 \qquad \theta_3 = \phi_2 + \phi_3. \end{aligned} \tag{3.5}$$

This new Hamiltonian is independent of ϕ_2 and therefore

$$\rho_2 = J_1 + J_2 + J_3 = N$$

is conserved. This essentially effectively reduces the dimension while introducing a parameter N.

The last canonical change of variables:

$$z_j = \sqrt{\rho_j} e^{i\phi_j} \; ; \; \bar{z}_j = \sqrt{\rho_j} e^{-i\phi_j} \tag{3.6}$$

leads to the Hamiltonian

$$H = -3|z_1|^2 + \frac{N}{6} H_{\text{quadratic}_1} + H_{\text{quartic}_1} + H.O.T. \tag{3.7}$$

(H.O.T. = higher order terms) with quadratic part

$$\begin{aligned} H_{\text{quadratic}_1} = 2\sqrt{2}\left(z_1\bar{z}_3 + z_3\bar{z}_1\right) - \left(|z_1|^2 - |z_3|^2\right) - \left(z_1 + z_3\right)^2 \\ - \left(\bar{z}_1 + \bar{z}_3\right)^2 + \left(1 + \sqrt{2}\right)\left(z_1 z_3 + \bar{z}_1\bar{z}_3\right) \end{aligned}$$

and quartic part

$$\begin{aligned} H_{\text{quartic}_1} = \frac{1}{4}|z_1|^4 - \frac{1}{6}|z_3|^4 + \frac{1}{6}|z_1|^2|z_3|^2 \\ - \frac{1}{6}\left(z_1^2\bar{z}_3^2 + \bar{z}_1^2 z_3^2\right) - (z_1\bar{z}_3 + \bar{z}_1 z_3)\left(\frac{\sqrt{2}}{3}|z_1|^2 + \frac{1}{\sqrt{2}}|z_3|^2\right) \\ - \frac{1}{12}\left(z_3^2 + \bar{z}_3^2\right)\left(|z_1|^2 + |z_3|^2\right) + \frac{1}{6}\left(z_1^2 + \bar{z}_1^2\right)\left(|z_1|^2 + |z_3|^2\right) \\ - \frac{1}{3\sqrt{2}}\left(z_1 z_3 + \bar{z}_1\bar{z}_3\right)\left(|z_1|^2 + |z_3|^2\right) \end{aligned}$$

which is independent of z_2 and $\bar{z}_2$ since they have been absorbed by the parameter N. We ignore a constant term $3N - \frac{N^2}{4}$, as it does not affect the dynamics. The above holds on the triangle

$$\{(\rho_1, \rho_3) \mid 0 < \rho_1 < N, 0 < \rho_3 < N, 0 < \rho_1 + \rho_3 < N\},$$

where ρ_1 and ρ_3 are given as the magnitudes of z_1 and z_3, respectively.

Note that any one choice of the z_j can be eliminated though a slightly different change of variables. In the case of the solution in Section 3.3.1, we choose to eliminate z_1 instead of z_2 and the following Hamiltonian arises after expanding the term $\sqrt{N - |z_2|^2 - |z_3|^2}$ by its Taylor series. Cubic terms arise from this expansion.

$$H = -\frac{N^2}{6} + H_{\text{quadratic}_2} + H_{\text{cubic}_2} + H_{\text{quartic}_2} + H.O.T. \tag{3.8}$$

where

$$H_{\text{quadratic}_2} = \frac{1}{6}\left[-N\left(z_2^2 + z_3^2 + \bar{z_2}^2 + \bar{z_3}^2\right) + (18 - 2N)\left(|z_2|^2 + |z_3|^2\right)\right] \tag{3.9}$$

$$H_{\text{cubic}_2} = \frac{\sqrt{2N}}{6}\left[z_2^2\bar{z}_3 + \bar{z}_2{}^2 z_3 + \left(2|z_2|^2 - |z_3|^2\right)(z_3 + \bar{z}_3)\right] \tag{3.10}$$

and

$$\begin{aligned} H_{\text{quartic}_2} = \frac{1}{12}\left[3\left(|z_2|^4 + |z_3|^4\right) + 8|z_2|^2|z_3|^2 - \left(z_2^2\bar{z}_3{}^2 + z_3^2\bar{z}_2{}^2\right)\right] \\ + \frac{1}{6}\left(|z_2|^2 + |z_3|^2\right)\left(z_2^2 + \bar{z}_2{}^2 + z_3^2 + \bar{z}_3{}^2\right) \end{aligned} \tag{3.11}$$

3.3 Analysis of the Standing Waves

The standing wave solutions (3.2)-(3.4) considered in the full space are now the fixed points in the reduced space. Linear stability analysis is used to learn how these solutions behave as the value of N changes. H is rewritten in a neighborhood of each solution z by letting $z = z^* + \widetilde{z}$, where z^* is each standing wave solution (3.2)-(3.4). The nodal solution, however, is the most interesting case and we need some additonal techniques to check how the solution behaves. This is explained in Subsection 3.3.3. For the defocusing DNLS, the case where the derivative term in equation (1.1) is the opposite of the sign of the nonlinear term, the solutions are the same, however, the stability of these solutions may change.

3.3.1 The Constant Solution

In the reduction resulting in the Hamiltonian (3.8), the constant solution (3.2) becomes

$$\mathbf{z_c} = \begin{pmatrix} z_2 \\ z_3 \end{pmatrix} = \begin{pmatrix} 0 \\ 0 \end{pmatrix}.$$

Note, the process is the same as in Subsection 3.2, though a different change of variables is used. In the reduced system, the quadratic part of H can be written as $\mathbf{z}^\top H\mathbf{z}$ where $z_j = \sqrt{2}x_j + i\sqrt{2}y_j$ i.e.,

$$\mathbf{z} = \begin{pmatrix} x_2 \\ x_3 \\ y_2 \\ y_3 \end{pmatrix}$$

and

$$L = JH_0 = 3\begin{pmatrix} 0 & 0 & 1 & 0 \\ 0 & 0 & 0 & 1 \\ \frac{1}{9}(-9+2N) & 0 & 0 & 0 \\ 0 & \frac{1}{9}(-9+2N) & 0 & 0 \end{pmatrix}, \tag{3.12}$$

where J is (2.3). L has eigenvalues

$$\lambda = \pm\frac{1}{3}\sqrt{-9+2N} \tag{3.13}$$

each with multiplicity two. Further analysis is provided in Chapter 5.

Critical values of N (points at which the dynamics of the solution change) occur when the sign under the square root changes for the eigenvalues of (3.12) and are $N_c = \frac{9}{2}$. At these values, $\lambda = 0$ has multiplicity four and it can be seen that transcritical bifurcation arises based on collisions of the above eigenvalues.

When $N < \frac{9}{2}$, eigenvalues are purely imaginary and of the form $\pm ai$ whereas when $N > \frac{9}{2}$, eigenvalues become real and have the form $\pm a$. We require the use of Poincaré-Lindstedt, mentioned in the appendix of this paper, for this problem.

3.3.2 The Vortex Solution

The vortex solution $\mathbf{\Psi}_v$ in (3.3) with z_2 eliminated corresponds to

$$\mathbf{z_v} = \begin{pmatrix} z_1 \\ z_3 \end{pmatrix} = \begin{pmatrix} 0 \\ -i\sqrt{\frac{N}{2}} \end{pmatrix}$$

in the reduced system. In this case,

$$L = JH_0 = \begin{pmatrix} 0 & 0 & -3 - \frac{N}{3} & -\frac{\sqrt{2}N}{3} \\ 0 & 0 & -\frac{\sqrt{2}N}{3} & -\frac{2N}{3} \\ 3 + \frac{N}{3} & -\frac{N}{3\sqrt{2}} & 0 & 0 \\ -\frac{N}{3\sqrt{2}} & \frac{N}{6} & 0 & 0 \end{pmatrix}$$

and the four eigenvalues are

$$\lambda = \pm \frac{\sqrt{\pm 3\sqrt{(9+4N)} - 9 - 2N}}{\sqrt{2}}.$$

The eigenvalues are purely imaginary for all values of $N > 0$, so no bifurcations arise and the solution (3.3) is surrounded by quasiperiodic orbits.

3.3.3 The Nodal Solution

The third solution (3.4) corresponds to the zero solution

$$\mathbf{z_n} = \begin{pmatrix} z_1 \\ z_3 \end{pmatrix} = \begin{pmatrix} 0 \\ 0 \end{pmatrix}$$

in the reduced system resulting from the change of variables associated with Hamiltonian (3.7) we obtain

$$L = JH_0 = \begin{pmatrix} 0 & 0 & -3+\frac{N}{6} & \frac{N}{3\sqrt{2}} \\ 0 & 0 & \frac{N}{3\sqrt{2}} & \frac{N}{3} \\ 3+\frac{N}{2} & -\frac{N}{\sqrt{2}} & 0 & 0 \\ -\frac{N}{\sqrt{2}} & 0 & 0 & 0 \end{pmatrix}$$

which has characteristic polynomial

$$P(\lambda) = \lambda^4 + \left(9 + N + \frac{N^2}{4}\right)\lambda^2 + \frac{N^3}{2} \tag{3.14}$$

with eigenvalues

$$\lambda = \pm\frac{\sqrt{-5N - 36 \pm \sqrt{-32N^3 + 25N^2 + 360N + 1296}}}{2\sqrt{2}}.$$

HH bifurcations occur at values of N for which the characteristic polynomial (3.14) has double roots on the imaginary axis. The double roots occur for two real critical values of N where the inner square root vanishes: $N_{H1} = 2 + \frac{4\left(\sqrt[3]{9-\sqrt{57}}+\sqrt[3]{9+\sqrt{57}}\right)}{3^{2/3}} \approx 9.077$ and $N_{H2} = 18$. Because the algebra is more tractable, we consider the bifurcation at N_{H2}, the larger critical value first. At $N = N_{H1}$ or $N = N_{H2}$, the matrix L has

double eigenvalues on the imaginary axis. For $N_{H1} < N < N_{H2}$, the eigenvalues form a quartet and the standing wave is unstable.

Bifurcations at $\mathbf{N_{H2}}$ At $N_{H2} = 18$, the system with P as in equation (A.3), and the matrix K_0 in (2.10) has $\sigma = 1$ and $\Omega = -3\sqrt{6}$. This comes from the canonical change of variables P as obtained using the Burgoyne-Cushman algorithm, explained in the Appendix A. When $N_{H2} = 18 + \delta$, the aforementioned change of variables yields the Hamiltonian of the form (2.9). The quadratic part of H is exactly (2.10) when the perturbation variable $\delta = 0$.

Letting new position vector $\boldsymbol{\xi}$ as in (2.8) then

$$H_2 = \boldsymbol{\xi}^\top K_0 \boldsymbol{\xi} = \frac{1}{2}\left(\xi_1^2 + \xi_2^2\right) + \Omega\left(\eta_2\xi_1 - \eta_1\xi_2\right), \tag{3.15}$$

$$\hat{H}_2 = \frac{1}{6}\eta_1\xi_1 - \frac{7\eta_1\xi_2}{12\sqrt{6}} + \frac{\eta_2\xi_1}{\sqrt{6}} + \frac{\eta_1^2}{4} + \frac{\xi_1^2}{12} + \frac{49\xi_2^2}{864} + \frac{5\xi_1\xi_2}{36\sqrt{6}}, \tag{3.16}$$

and

$$\begin{aligned} H_4 = &-\frac{1}{4}\eta_1^3\xi_1 + \frac{7\eta_1^3\xi_2}{8\sqrt{6}} - \frac{5}{24}\eta_1^2\xi_1^2 - \frac{49}{192}\eta_1^2\xi_2^2 - \frac{1}{2}\sqrt{\frac{3}{2}}\eta_2\eta_1^2\xi_1 + \frac{1}{8}\sqrt{\frac{3}{2}}\eta_1^2\xi_1\xi_2 \\ &-\frac{1}{12}\eta_1\xi_1^3 + \frac{535\eta_1\xi_2^3}{1728\sqrt{6}} - \frac{\eta_2\eta_1\xi_1^2}{\sqrt{6}} + \frac{1}{3}\sqrt{\frac{2}{3}}\eta_2\eta_1\xi_2^2 - \frac{91}{864}\eta_1\xi_1\xi_2^2 + \frac{\eta_2^2\eta_1\xi_2}{\sqrt{6}} \\ &+\frac{41\eta_1\xi_1^2\xi_2}{108\sqrt{6}} + \frac{7}{36}\eta_2\eta_1\xi_1\xi_2 - \frac{61\eta_2\xi_1^3}{108\sqrt{6}} + \frac{1}{27}\eta_2\xi_2^3 - \frac{5}{18}\eta_2^2\xi_1^2 + \frac{1}{18}\eta_2^2\xi_2^2 \\ &-\frac{203\eta_2\xi_1\xi_2^2}{432\sqrt{6}} - \frac{1}{3}\sqrt{\frac{2}{3}}\eta_2^3\xi_1 - \frac{13}{108}\eta_2\xi_1^2\xi_2 - \frac{\eta_2^2\xi_1\xi_2}{3\sqrt{6}} - \frac{3\eta_1^4}{16} - \frac{341\xi_1^4}{11664} \\ &-\frac{865\xi_2^4}{248832} - \frac{5\xi_1\xi_2^3}{64\sqrt{6}} - \frac{683\xi_1^2\xi_2^2}{15552} - \frac{5\xi_1^3\xi_2}{324\sqrt{6}}. \end{aligned} \tag{3.17}$$

While the leading order term H_2 is now quite simple, the dynamics are not at all obvious from (3.16) and (3.17). We want to simplify $\hat{H}_2$ and H_4 as much as possible. This is achievable by computing a projection for this system. Some of the terms in the normal form will be removable through the projection technique which we explain below.

First, it is important to note that $\hat{H}_2$ and H_4 are elements of vector spaces of homogeneous quadratic and quartic monomials, respectively

$$P_0^{(m)}\left(\mathbb{R}^4\right) = \text{Span}\{{\xi_1}^i {\xi_2}^j {\eta_1}^k {\eta_2}^l | i+j+k+l=m\}.$$

These have dimension $\dim(P_0^{(2)}(\mathbb{R}^4)) = 10$ and $\dim(P_0^{(4)}(\mathbb{R}^4)) = 35$.

The algorithm is explained in Meyer and Hall [27] using the adjoint operator $ad_{H_2}^{(m)}(\circ) = \{\circ, H_2\}$, a linear mapping from $P_0^{(m)}$ to $P_0^{(m)}$. From the Fredholm Alternative, we can decompose $P_0^{(m)}(\mathbb{R}^4) = \text{Range}(ad_{H_2}^{(m)}) \bigoplus \text{Null}(ad_{H_2}^{(m)})^\top$. The resonant terms which cannot be removed, lie in $\text{Null}(ad_{H_2}^{(m)})^\top$, while the nonresonant terms which can be removed, lie in $\text{Range}(ad_{H_2}^{(m)})$. In $\mathbb{R}^{10}$ and $\mathbb{R}^{35}$, $ad_{H_2}^{(m)}$ is equivalent to matrix-vector multiplication.

Using the above, we algorithmically compute projections of $P_0^{(m)}$ onto $\text{Null}(ad_{H_2}^{(m)})^\top$ in *Mathematica*. Specifically, we write (3.16) and (3.17) as vectors in $\mathbb{R}^{10}$ and $\mathbb{R}^{35}$ then project them onto the nullspace.

In order to compute the projection, let us first define the natural inner product. The inner product of any two vectors ξ and η belonging to the real vector space V is

defined as

$$\langle \xi, \eta \rangle = \sum_{i=1}^{m} \xi_i \eta_i \omega_i$$

where $\xi = (\xi_1, \xi_2, ..., \xi_m), v = (\eta_1, \eta_2, ..., \eta_m) \in \mathbb{R}^m$ and ω_i are the weights associated with the monomials. That is, for the term $\xi_1\eta_2$ the weight is $\omega = 2$ but for ξ_1^2 the weight is $\omega = 1$. Inner products have properties of linearity, symmetry and positive definiteness.

The projection is defined as

$$Proj_{\mathrm{Null}(ad_{H_2}^{(m)})^\top} P_0^{(m)} = \frac{\left\langle \mathrm{Null}(ad_{H_2}^{(m)})^\top, P_0^{(m)} \right\rangle}{\left\langle \mathrm{Null}(ad_{H_2}^{(m)})^\top, \mathrm{Null}(ad_{H_2}^{(m)})^\top \right\rangle} \mathrm{Null}(ad_{H_2}^{(m)})^\top \tag{3.18}$$

This gives us the normal form with the resonant terms of the Hamiltonian (2.9) with (3.15)–(3.17).

The resonant normal form Hamiltonian can nicely be written in terms of the three combinations of

$$\Gamma_1 = \xi_2\eta_1 - \xi_1\eta_2, \Gamma_2 = \frac{1}{2}(\xi_1^2 + \xi_2^2), \Gamma_3 = \frac{1}{2}(\eta_1^2 + \eta_2^2).$$

The combinations Γ_1 and Γ_2 appear in H_2 and Γ_1 and Γ_3 span $\mathrm{Null}(ad_{H_2}^{(2)})^\top$. Higher order terms make up the normal form if they are functions of only Γ_1 and Γ_3. The general form is

$$H(\delta) = \Omega\Gamma_1 + \sigma\Gamma_2 + \delta(a\Gamma_1 + b\Gamma_3) + \frac{1}{2}(c\Gamma_1^2 + 2d\Gamma_1\Gamma_3 + e\Gamma_3^2) + O(3), \tag{3.19}$$

where $O(3)$ indicates terms $\delta^j \Gamma^k$ for $j+k=3$. We follow assumptions that $\Omega \neq 0$, $\sigma = \pm 1$, $b \neq 0$ and $e \neq 0$. For N_{H2},

$$\Omega = -3\sqrt{6}, \sigma = 1, a = -\frac{19\sqrt{6}}{24}, b = \frac{1}{4}, c = -\frac{121}{72}, d = -\frac{19}{32}\sqrt{\frac{3}{2}}, e = -\frac{9}{16}.$$

At this point, we quote a result by Meyer and Hall. The next step is the Poincaré-Lindstedt expansion, a method used to construct periodic orbits of "amplitude" r and frequency $(1+\tau)\,\Omega$ [27]. Carrying through the expansion shows that the variables τ and r satisfy the equation

$$\Omega^2 \tau^2 - \sigma e r^2 = \sigma b \nu.$$

Depending on the sign of σe, the families of periodic orbits are hyperbolic or elliptic. These are the two types of the HH bifurcation and are determined by the quadratic form. It is found $\sigma e < 0$, so for $N_{H2} = 18$, the elliptic case in Figure 2.3 arises as was discussed earlier in Section 2.3.

Bifurcations at $\mathbf{N_{H1}}$ The same analysis can be performed in a neighborhood of $N_{H1} \approx 9.077$. For this case,

$$\Omega = \sqrt{\frac{2}{3}\left(13 + \left(514 - 6\sqrt{57}\right)^{\frac{1}{3}} + \left(514 + 6\sqrt{57}\right)^{\frac{1}{3}}\right)} \approx 4.39749,$$

with P is as in equation (A.2), and the matrix K_0 in (2.10), has $\sigma = 1$. While it may be possible to proceed analytically, we choose to determine the type of HH

numerically. The Hamiltonian in (3.19) has values

$$\omega = -\Omega, \sigma = -1, a = -0.339107, b = 0.21315,$$

$$c = 2.142945, d = -6.2065, e = -0.35638,$$

thus $\sigma e > 0$ and the HH bifurcation is of the hyperbolic type. The families meet at the origin and become one. They continue to move further out along the horizontal axis, when $N_{H1} < N < N_{H2}$. When N crosses though N_{H2}, another branch forms and is the elliptic case. The branch starts out as a point at the origin when $N = N_{H2}$, and as the parameter N is increased further, the ellipse expands in each direction. The branch formed at $N = N_{H1}$ continues to exist for $N > N_{H2}$; it has just moved very far away from the origin and continues to do so in the horizontal direction as N keeps increasing.

CHAPTER 4

NUMERICAL INVESTIGATION OF THE NODAL SOLUTION

For the nodal solution (3.4), H is of the form (3.19). Meyer and Hall [27] make the following scalings so that yet another symplectic change of variables (used also by [10]) can be used to reduce once more.

We begin by making scalings

$$\begin{aligned} \xi_1 &= \epsilon^2 \xi_1 \qquad \xi_2 = \epsilon^2 \xi_2 \qquad \delta = \epsilon^2 \delta \\ \eta_1 &= \epsilon \eta_1 \qquad \eta_2 = \epsilon \eta_2. \end{aligned} \tag{4.1}$$

This change is symplectic with multiplier ϵ^3. The matrix L is put into normal form by applying the symplectic polar change of variables

$$\begin{aligned} \xi_1 &= r\cos\theta \qquad \eta_1 = R\cos\theta - \frac{\Theta}{r}\sin\theta \\ \xi_2 &= r\sin\theta \qquad \eta_2 = R\sin\theta + \frac{\Theta}{r}\cos\theta \end{aligned} \tag{4.2}$$

to the linear and quadratic part of the Hamiltonian of form (3.19). A very similar polar change of variables is done by Lahiri, where this change allows for identifications of fast and slow variables [23].

The Hamiltonian in (3.19) is now

$$H = \Theta\Omega + \frac{\epsilon\left(4b\delta r^4 + er^6 + 4\sigma\left(\Theta^2 + r^2R^2\right)\right)}{8r^2} + O(\epsilon^2) \tag{4.3}$$

The $\mathcal{O}(1)$ part is just a constant and merely describes the decoupled evolution of θ.

It is found in our problem that there is no dependence on θ and that Θ is a constant. This allows for a reduction of the system to just r and R. The numerical investigation is carried out in two ways: one, by investigating the system's solutions for different parameter values of e, δ, b, σ and Θ (where e, δ and σ will correspond to each critical case of N) and two, by finding the associated Poincaré Map.

4.1 Phase Plane of the Nodal Solution

We are interested in the $\mathcal{O}(\epsilon)$ part of (4.3) which is

$$H_\epsilon(r, R) = \frac{1}{2}b\delta r^2 + \frac{er^4}{8} + \frac{\Theta^2\sigma}{2r^2} + \frac{R^2\sigma}{2}.$$

Note that H_ϵ in (4.1) is of the form $\frac{\sigma R^2}{2} + V(r)$ where $V(r)$ is the potential. This indicates that $\frac{d^2r}{dt^2} + \frac{V'(r)}{\sigma} = 0$. From H_ϵ, we derive equations for $\dot{r}$ and $\dot{R}$:

$$\begin{aligned}\dot{r} &= R\sigma \\ \dot{R} &= -\frac{2b\delta r^4 + er^6 - 2\Theta^2\sigma}{2r^3}\end{aligned}$$

Plotting the potential function

$$V(r) = \frac{\Theta^2}{2r^2} + \frac{1}{2}b\delta r^2\sigma + \frac{1}{8}\sigma e r^4$$

mentioned above would be equivalent to plotting nullclines.

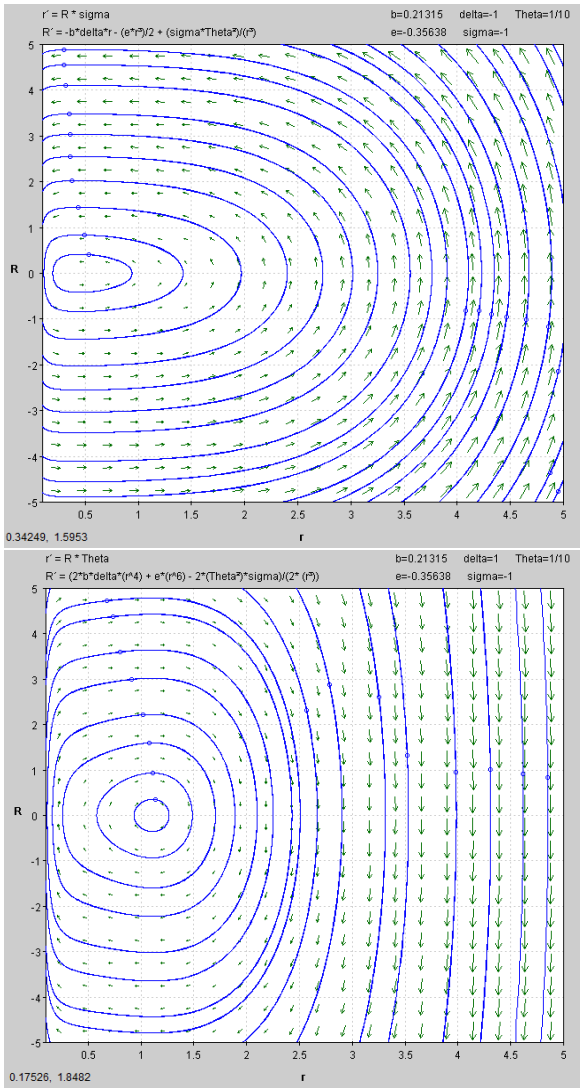

Figure 4.1 $N \approx 9.077$ with $\Theta = \frac{1}{10}$. (a) $\delta < 0$ (b) $\delta > 0$: center moves on the positive r axis.

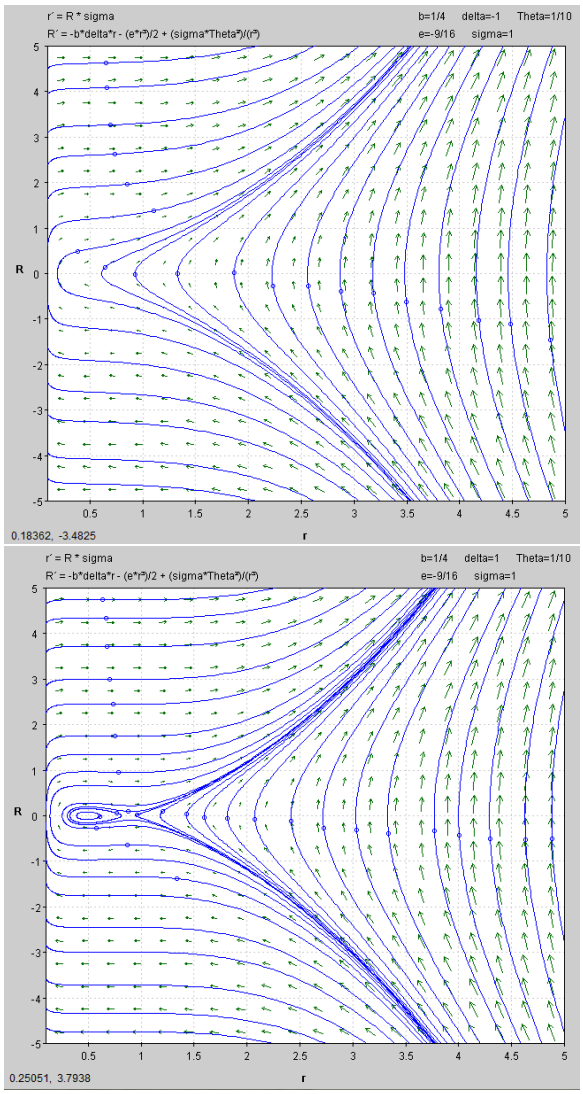

Figure 4.2 N=18 with $\Theta = \frac{1}{10}$. (a) $\delta < 0$ (b) $\delta > 0$: center appears on the positive r axis.

The software *pplane* is used to investigate the phase space from equations for $\dot{r}$ and $\dot{R}$ as values for Θ and δ are changed.

As $|\Theta|$ gets larger, the phase plane is stretched more vertically, however, the sign of δ is what changes the dynamics. It is important to note that the asymptote at $r = 0$ exists because a $\frac{1}{r}$ term is introduced in the definition for η_1 and η_2 in equation (4.2), but does not exist in the original problem. We consider values $r > 0$.

For $N \approx 9.077$, when $\delta < 0$, a center exists, but as $\delta > 0$, the center moves on the positive r axis, shifting rightward. See Figures 4.1a and 4.1b, respectively. This problem could be investigated further as there are no different dynamics that can be seen from this approach for changing values of δ. For $N = 18$, it can be seen for $\delta < 0$, there are no fixed points but for $\delta > 0$ there is a center on the positive r axis. See Figures 4.2a and 4.2b, respectively. It is the $\Theta = 0$ case where different dynamics can be seen.

4.2 Poincaré Map for the Nodal Solution

Next, we compute Poincaré Maps for values of N near the critical values (recall $N \approx 9.077$ and $N = 18$) in Matlab. The system in terms of $(\xi_1, \xi_2, \eta_1, \eta_2)$ is used and we plot the ODEs for solutions very near $(\xi_1, \xi_2, \eta_1, \eta_2) = (0, 0, 0, 0)$. See Figures 4.3–4.6. To plot the Poincaré Map of the system corresponding to the nodal solution (3.4), we evolve the system numerically and take a "snapshot" of (ξ_1, η_1) whenever $\eta_2 = 0$. The numerical results are as expected. For $N = 17.9$, the Poincaré Map shows chaos Figure 4.6a, and for $N = 9$, $N = 9.1$, and $N = 18.1$, the plots imply quasiperiodic orbits. Additional numerics are needed in order to see how the dynamics change as

we perturb $N = 9.077 + \delta\epsilon$, where $\delta = \pm 1$ and $\epsilon > 0$ and small. See Figures 4.4a, 4.4b and 4.6b, respectively.

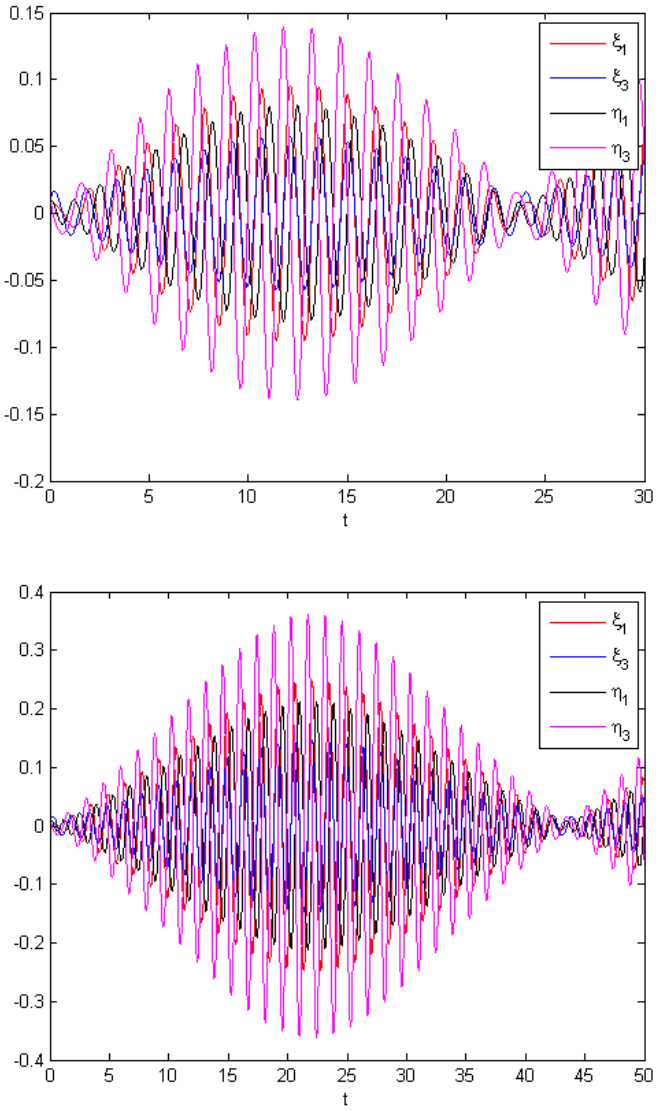

Figure 4.3 Solutions of ξ_1, ξ_3, η_1 and η_3. (a) For $N = 9$. (b) For $N = 9.1$.

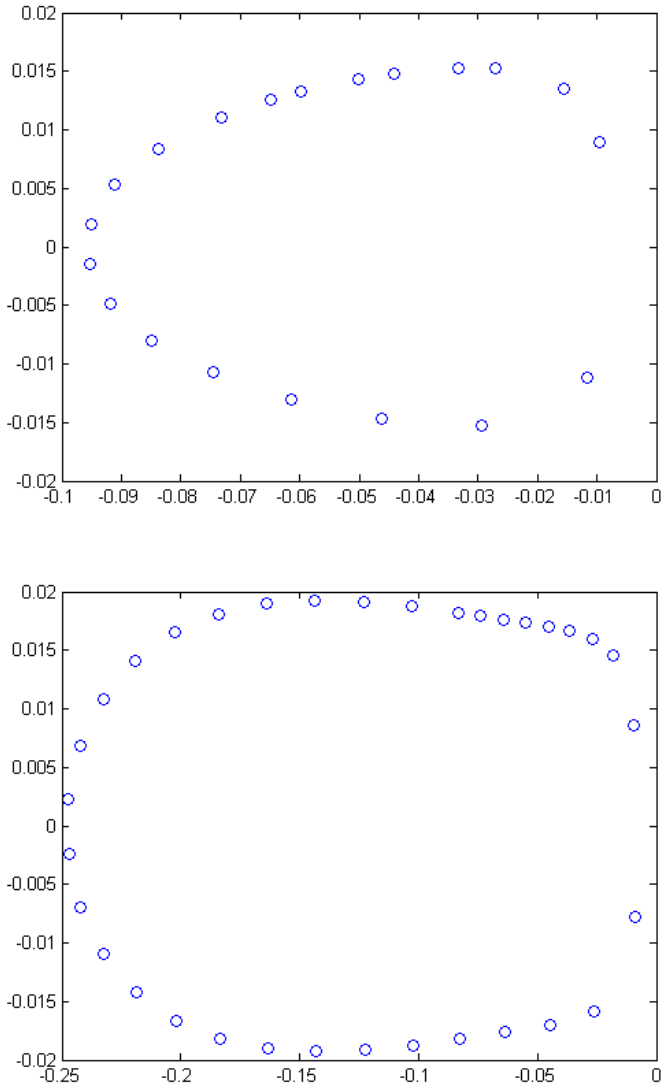

Figure 4.4 Poincaré maps (a) For $N = 9$. (b) For $N = 9.1$.

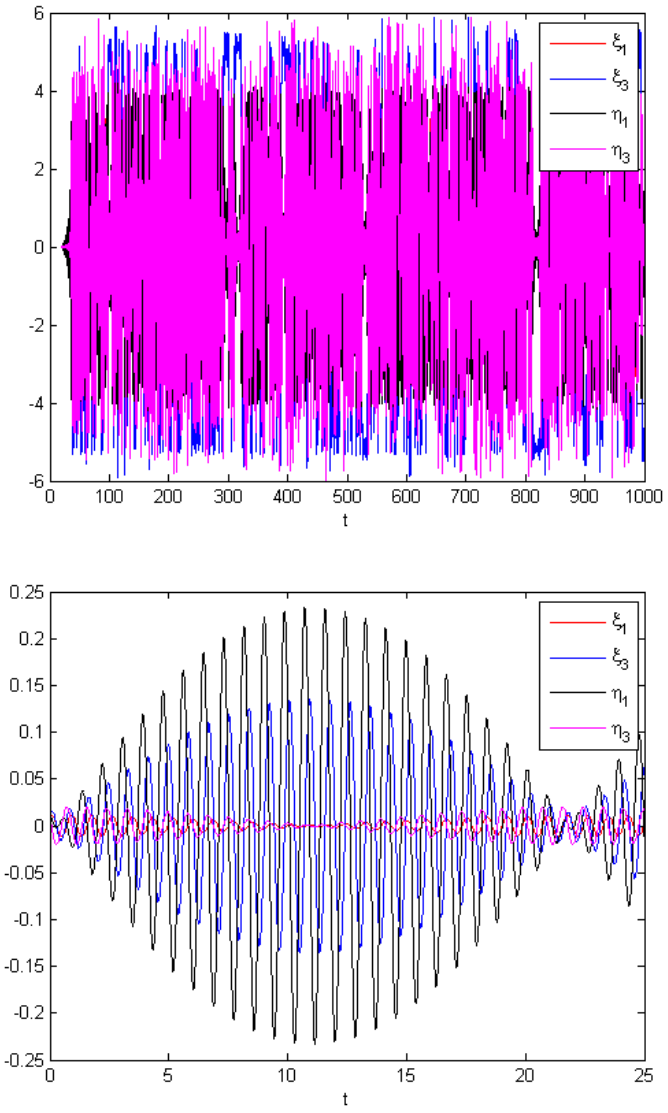

Figure 4.5 Solutions of ξ_1, ξ_3, η_1 and η_3. (a) For $N = 17.9$. (b) For $N = 18.1$.

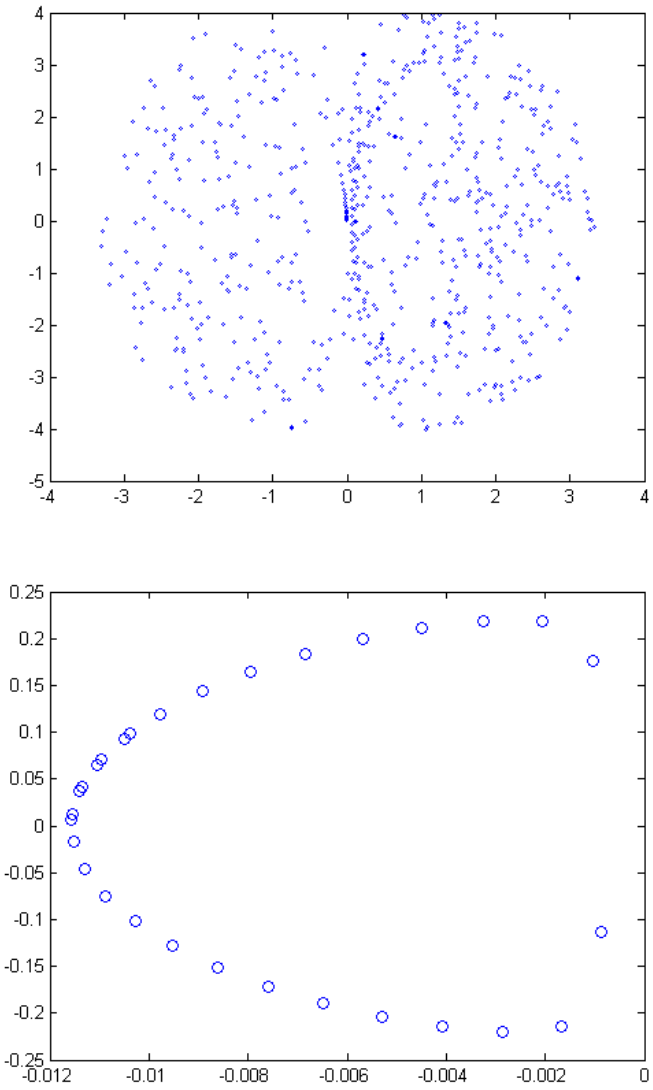

Figure 4.6 Poincaré maps (a) for $N = 17.9$ and (b) for $N = 18.1$.

CHAPTER 5

ANALYSIS NEAR THE CONSTANT SOLUTION

5.1 The Constant Solution

We now investigate the stability and dynamics of the constant solution (3.2). To examine the dynamics near this solution, the system is reduced to two degrees of freedom, as was done previously for the HH bifurcation. This time we choose to eliminate z_1 and $\bar{z_1}$ rather than z_2 and $\bar{z_2}$ so that this solution corresponds to the zero solution $(z_2, z_3, \bar{z_2}, \bar{z_3}) = (0, 0, 0, 0)$. The following change of variables is used in place of (3.5)

$$
\begin{aligned}
J_1 &= \rho_1 - \rho_2 - \rho_3 & J_2 &= \rho_2 & J_3 &= \rho_3 \\
\theta_1 &= \phi_1 & \theta_2 &= \phi_1 + \phi_2 & \theta_3 &= \phi_1 + \phi_3
\end{aligned}
$$

and results in the Hamiltonian

$$
\begin{aligned}
H = &\left(3 - \frac{N}{3}\right)\left(|z_2|^2 + |z_3|^2\right) - \frac{N}{6}\left(N + z_2^2 + z_3^2 + \bar{z_2}^2 + \bar{z_3}^2\right) \\
&+ \frac{\sqrt{N - |z_2|^2 - |z_3|^2}}{3\sqrt{2}}\left(z_2^2\bar{z_3} + \bar{z_2}^2 z_3 + \left(2|z_2|^2 - |z_3|^2\right)\left(z_3 + \bar{z_3}\right)\right) \\
&+ \frac{1}{4}\left(|z_2|^4 + |z_3|^4\right) + \frac{1}{6}\left(|z_2|^2 + |z_3|^2\right)\left(z_2^2 + \bar{z_2}^2 + z_3 + \bar{z_3}^2\right) \\
&- \frac{1}{12}\left(z_2^2\bar{z_3}^2 + \bar{z_2}^2 z_3^2 + 8|z_2|^2|z_3|^2\right)
\end{aligned}
\tag{5.1}
$$

under the assumption $|z_2|^2, |z_3|^2 < N$. A Taylor Series expansion of the root term is required to see terms order by order in the perturbation.

$$\begin{aligned} H = &- \frac{N^2}{6} + 3\left(|z_2|^2 + |z_3|^2\right) - \frac{N}{6}\left(z_2^2 + z_3^2 + 2\left(|z_2|^2 + |z_3|^2\right) + \bar{z}_2^2 + \bar{z}_3^2\right) \\ &+ \frac{\sqrt{2N}}{6}\left[z_2^2\bar{z}_3 + z_3\bar{z}_2{}^2 + \left(2|z_2|^2 - |z_3|^2\right)(z_3 + \bar{z}_3)\right] \\ &+ \frac{1}{12}\left[3\left(|z_2|^4 + |z_3|^4\right) + 8|z_2|^2|z_3|^2 - z_2^2\bar{z}_3{}^2 - \bar{z}_2{}^2 z_3^2\right] \\ &+ \frac{1}{6}\left(|z_2|^2 + |z_3|^2\right)\left(z_2^2 + \bar{z}_2{}^2 + z_3^2 + \bar{z}_3{}^2\right) + O\left(|z|^5\right) \end{aligned} \tag{5.2}$$

We obtain a leading order linear system $\dot{\vec{x}} = L\vec{x}$ where $z_j = \frac{x_j + iy_j}{\sqrt{2}}$, $\bar{z}_j = \frac{x_j - iy_j}{\sqrt{2}}$ for $j = 2, 3$, $\vec{x} = (x_2, x_3, y_2, y_3)$ and

$$L = JH_0 = \begin{pmatrix} 0 & 0 & 3 & 0 \\ 0 & 0 & 0 & 3 \\ \frac{1}{3}(2N-9) & 0 & 0 & 0 \\ 0 & \frac{1}{3}(2N-9) & 0 & 0 \end{pmatrix}. \tag{5.3}$$

As can be seen in Equation (3.13), the critical value for N is $N = \frac{9}{2}$ where the eigenvalues go from pure imaginary pairs of multiplicity two for $N < \frac{9}{2}$ to pure real pairs of multiplicity two for $N > \frac{9}{2}$. The eigenvalues associated with this problem at the critical value for N are zero with multiplicity four.

For the constant solution (3.2), we have that

$$H_2 = \frac{3}{2}\left(\eta_1^2 + \eta_2^2\right) \tag{5.4}$$

The resonant terms of $\text{Null}(ad_{H_2})^\top$ are composed of products of ξ_1, ξ_2, and $\Gamma = \eta_2\xi_1 - \eta_1\xi_2$.

We perturb the parameter N by $N = \frac{9}{2} - \delta$ since in the next section, we are concerned with the periodic orbits of the system, which only occurs when the eigenvalues of the matrix L in (5.3) are pure imaginary. The Hamiltonian is a result of using scalings $\xi_1 \to \delta\xi_1$, $\xi_2 \to \delta\xi_2$, $\eta_1 \to \delta\eta_1$ and $\eta_2 \to \delta\eta_2$, then dividing by a factor of δ^2, and is a normal form calculated through the use of Lie Transforms.

This Hamiltonian only contains resonant terms, and a similar projection as in Subsection 3.3.3 is used, however this time, there are cubic terms in addition to quadratic and quartic. These cubic terms arise from the Taylor expansion of $\sqrt{N - |z_2|^2 - |z_3|^2}$ in equation (5.1).

$$\begin{aligned} H_{\frac{9}{2}} =& \frac{3}{2}\left(\eta_1^2 + \eta_2^2\right) + \frac{\delta}{3}\left(\xi_1^2 + \xi_2^2\right) + \frac{\delta^2}{2\sqrt{2}}\xi_2\left(3\xi_1^2 - \xi_2^2\right) - 3\frac{\delta^3}{\sqrt{2}}\xi_2\left(3\xi_1^2 - \xi_2^2\right) \\ &+ \delta^4\left(\frac{1}{12}\left(\xi_1^2 + \xi_2^2\right)^2 + \frac{5}{24}\left(\eta_2\xi_1 - \eta_1\xi_2\right)^2 + \frac{\xi_2\left(3\xi_1^2 - \xi_2^2\right)}{324\sqrt{2}}\right) + O\left(\delta^5\right) \end{aligned} \tag{5.5}$$

Terms are calculated to fourth order in δ because we may need to carry perturbation to third order to find the quantities that determine the behavior. The corresponding

system is

$$\begin{aligned}
\dot{\xi_1} &= 3\eta_1 + \frac{5}{12}\delta^4\xi_2\left(\eta_1\xi_2 - \eta_2\xi_1\right) \\
\dot{\xi_2} &= 3\eta_2 + \frac{5}{12}\delta^4\xi_1\left(\eta_2\xi_1 - \eta_1\xi_2\right) \\
\dot{\eta_1} &= -\frac{2}{3}\delta\xi_1 - \frac{3}{\sqrt{2}}\delta^2\xi_1\xi_2 + \frac{1}{3}\sqrt{2}\delta^3\xi_1\xi_2 \\
&\quad + \delta^4\left(\frac{5}{12}\eta_2\left(\eta_2\xi_1 - \eta_1\xi_2\right) + \frac{\xi_1\xi_2}{54\sqrt{2}} + \frac{1}{3}\xi_1\left(\xi_1^2 + \xi_2^2\right)\right) \\
\dot{\eta_2} &= -\frac{2}{3}\delta\xi_2 + \frac{3}{2\sqrt{2}}\delta^2\left(\xi_2^2 - \xi_1^2\right) - \frac{1}{3\sqrt{2}}\delta^3\left(\xi_2^2 - \xi_1^2\right) \\
&\quad - \delta^4\left(\frac{5}{12}\eta_1\left(\eta_1\xi_2 - \eta_2\xi_1\right) + \frac{1}{3}\xi_2\left(\xi_1^2 + \xi_2^2\right) - \frac{\xi_2^2 - \xi_1^2}{108\sqrt{2}}\right)
\end{aligned}$$

If we calculate the system corresponding to $H_{\frac{9}{2}}$ as in equation (5.5) *without* the scalings, we can rewrite the system up to $O(\delta^3)$ as a pair of spring equations, i.e. two second order ODEs.

$$\begin{aligned}
\frac{3}{2}\ddot{\xi_1} + \frac{2\delta}{3}\xi_1 + \frac{3}{2\sqrt{2}}\xi_1\xi_2 &= O\left(\delta^3\right) \\
\frac{3}{2}\ddot{\xi_2} + \frac{2\delta}{3}\xi_2 + \frac{3}{2\sqrt{2}}\left(\xi_1^2 - \xi_2^2\right) &= O\left(\delta^3\right)
\end{aligned} \tag{5.6}$$

The system has four fixed points $(\xi_1, \xi_2) = (0, 0)$, $(\xi_1, \xi_2) = (0, \frac{4\sqrt{2}\delta}{9})$, $(\xi_1, \xi_2) = (\frac{8\delta}{9}, -\frac{4\sqrt{2}\delta}{9})$ and $(\xi_1, \xi_2) = (\frac{8\delta}{9}, -\frac{4\sqrt{2}\delta}{9})$. The multiplicity of three has to be the case due to the symmetries of the system [11]. This type of bifurcation at $(\xi_1, \xi_2) = (0, 0)$ is called a symmetric transcrititcal bifurcation because there are two symmetric branches and can be seen in Figure 5.1. Essentially the same Poincaré-Lindstedt calculation as in Section 5.2 could be carried out for solutions $(\xi_1, \xi_2) = (\frac{8\delta}{9}, -\frac{4\sqrt{2}\delta}{9})$ and $(\xi_1, \xi_2) = (\frac{8\delta}{9}, -\frac{4\sqrt{2}\delta}{9})$, but at $N = \frac{9}{2} + \delta$ rather than $N = \frac{9}{2} - \delta$, since this is

where periodic orbits take place for these solutions. The phase portrait of (ξ_2, η_2) for the solution $(\xi_1, \xi_2) = (0, \frac{4\sqrt{2}\delta}{9})$ is that of the classic undamped pendulum.

5.2 Perturbative Calculation of Periodic Orbits

We use a Poincaré-Lindstedt expansion to investigate the reduced system without z_1. The system is first scaled with $\xi_j \to \xi_j$ and $\eta_j \to \sqrt{\delta}\eta_j$, for $j = 1, 2$, then dividing by $\sqrt{\delta}$. This makes the leading part of the same order.

$$\dot{\xi_1} = 3\eta_1 - \frac{5}{12}\delta^4 \xi_2 \left(\eta_2\xi_1 - \eta_1\xi_2\right)$$

$$\dot{\xi_2} = 3\eta_2 + \frac{5}{12}\delta^4 \xi_1 \left(\eta_2\xi_1 - \eta_1\xi_2\right)$$

$$\begin{aligned}\dot{\eta_1} = &-\frac{2\xi_1}{3} - \frac{3\delta\xi_1\xi_2}{\sqrt{2}} + \frac{1}{3}\sqrt{2}\delta^2\xi_1\xi_2 - \frac{1}{108}\delta^3\xi_1\left(36\left(\xi_1^2 + \xi_2^2\right) + \sqrt{2}\xi_2\right) \\ &+ \delta^4\left(-\frac{5}{12}\eta_2\left(\eta_2\xi_1 - \eta_1\xi_2\right) - \frac{5}{216}\xi_1\left(\xi_1^2 + \xi_2^2\right)\right)\end{aligned}$$

$$\begin{aligned}\dot{\eta_2} = &-\frac{2\xi_2}{3} - \frac{3\delta}{2\sqrt{2}}\left(\xi_1^2 - \xi_2^2\right) + \frac{\delta^2}{3\sqrt{2}}\left(\xi_1^2 - \xi_2^2\right) - \delta^3\left(\frac{\left(\xi_1^2 - \xi_2^2\right)}{108\sqrt{2}} + \frac{1}{3}\xi_2\left(\xi_1^2 + \xi_2^2\right)\right) \\ &- \delta^4\left(\frac{5}{12}\eta_1\left(\eta_1\xi_2 - \eta_2\xi_1\right) + \frac{5}{216}\xi_2\left(\xi_1^2 + \xi_2^2\right)\right)\end{aligned}$$

Notice the choice for the perturbation $N = N_c - \delta$ since we consider periodic orbits at the origin. The Poincaré-Lindstedt expansion could be performed on the system at the other solutions for $(\xi_1, \xi_2) = (\frac{8\delta}{9}, -\frac{4\sqrt{2}\delta}{9})$ and $(\xi_1, \xi_2) = (\frac{8\delta}{9}, -\frac{4\sqrt{2}\delta}{9})$ with $N = N_c + \delta$ as briefly mentioned in Section 5.1.

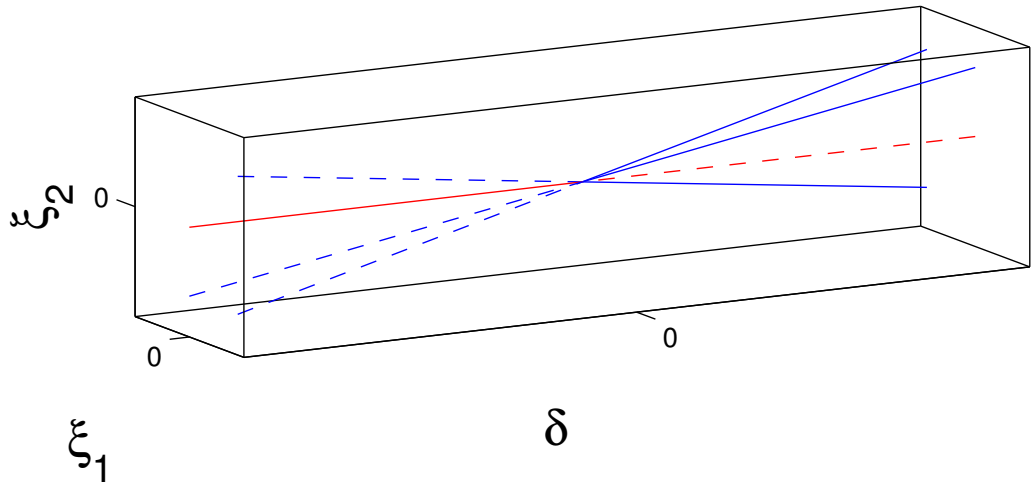

Figure 5.1 The symmetric transcritical bifurcations for the ξ_1 and ξ_2 solutions. Solid lines represent stability and dashed lines represent instability.

When using the Poincaré-Lindstedt method, the frequency is expanded as $\omega = \omega_0 + \delta\omega_1 + \delta^2\omega_2 + ...$, time is changed to $\tau = \omega t$, and $\xi_1 = \xi_{10} + \delta\xi_{11} + \delta^2\xi_{12} + ...$, $\xi_2 = \xi_{20} + \delta\xi_{21} + \delta^2\xi_{22} + ...$ $\eta_1 = \eta_{10} + \delta\eta_{11} + \delta^2\eta_{12} + ...$ and $\eta_2 = \eta_{20} + \delta\eta_{21} + \delta^2\eta_{22} + ...$ are expended. The system is broken up order by order and the coefficients are chosen to make secular terms equal to zero. The phase condition is

$$\mathbf{x}(0) = \boldsymbol{\alpha} = \begin{pmatrix} \alpha \\ a \\ \beta \\ b \end{pmatrix}$$

where $\alpha = \alpha_0 > 0$, $\beta = 0$ and expanded $a = a_0 + \delta a_1 + ...$ and $b = b_0 + \delta b_1 + ...$ are to be determined. The constant α_1 can be set to zero because we can assume all of the nontrivial parts of the initial condition are included at leading order. Including nonzero α_1 does not give a way to remove resonances, so we choose to ignore it for simplicity.

At leading order,

$$(\omega_0 \frac{d}{dt} - A)\mathbf{x}_0 = \vec{0}$$

where

$$A = L(\frac{9}{2} - \delta) = \begin{pmatrix} 0 & 0 & 3 & 0 \\ 0 & 0 & 0 & 3 \\ -\frac{2}{3} & 0 & 0 & 0 \\ 0 & -\frac{2}{3} & 0 & 0 \end{pmatrix}.$$

The general solution is

$$\mathbf{x}_0 = e^{\frac{At}{\omega_0}}\mathbf{x}_0(0)$$

Clearly at this order, to make the solution 2π periodic we require $\omega_0 = \sqrt{2}$.

Equating terms of order δ leads to the following system.

$$(\omega_0\frac{d}{dt} - A)\mathbf{x}_1 = -\omega_1\frac{d\mathbf{x}_0}{dt} + \begin{pmatrix} 0 \\ 0 \\ -\frac{3}{\sqrt{2}}\xi_{10}(t)\xi_{20}(t) \\ -\frac{3\sqrt{2}}{4}\left(\xi_{10}^2(t) - \xi_{20}^2(t)\right) \end{pmatrix}$$

At each order, the only option is to rid the solution of secular terms, resonant parts of each of the general solutions. This is required to keep solutions from blowing up as t tends to infinity. At $O(\delta)$, besides a trivial solution $\alpha_0 = 0$, we require that $\omega_1 = 0$. The solutions that satisfy the initial condition $\eta_1(0) = 0$ are

$$\begin{aligned}
\xi_{11} &= -\frac{9a_0\alpha_0}{4} + \frac{3}{2}a_0\alpha_0\cos(t) - \frac{9\alpha_0 b_0\sin(t)}{2\sqrt{2}} + \frac{3}{4}a_0\alpha_0\cos(2t) + \frac{9\alpha_0 b_0\sin(2t)}{4\sqrt{2}} \\
\xi_{21} &= \frac{9a_0^2}{8} - \frac{9\alpha_0^2}{8} + \frac{81b_0^2}{16}\frac{1}{4}\cos(t)\left(-3a_0^2 + 3\alpha_0^2 + 4a_1 - 27b_0^2\right) + \frac{3\left(3a_0b_0 + 2b_1\right)\sin(t)}{2\sqrt{2}} \\
&\quad + \frac{3}{16}\cos(2t)\left(-2a_0^2 + 2\alpha_0^2 + 9b_0^2\right) - \frac{9a_0b_0\sin(2t)}{4\sqrt{2}} \\
\eta_{11} &= -\frac{3}{2}\alpha_0 b_0\cos(t) - \frac{a_0\alpha_0\sin(t)}{\sqrt{2}} + \frac{3}{2}\alpha_0 b_0\cos(2t) - \frac{a_0\alpha_0\sin(2t)}{\sqrt{2}} \\
\eta_{21} &= +\frac{1}{2}\left(3a_0b_0 + 2b_1\right)\cos(t) - \frac{\left(-3a_0^2 + 3\alpha_0^2 + 4a_1 - 27b_0^2\right)\sin(t)}{6\sqrt{2}} \\
&\quad - \frac{3}{2}a_0b_0\cos(2t) - \frac{\left(-2a_0^2 + 2\alpha_0^2 + 9b_0^2\right)\sin(2t)}{4\sqrt{2}}.
\end{aligned}$$

The system for ξ_{12}, ξ_{22}, η_{12} and η_{22} is obtained by equating the $O(\delta^2)$ terms and is

$$(\omega_0\frac{d}{dt}-A)\mathbf{x}_2=-\omega_2\frac{d\mathbf{x}_0}{dt}$$
$$+\begin{pmatrix}0\\0\\\frac{1}{3}\sqrt{2}\xi_{10}(t)\xi_{20}(t)-\frac{3}{\sqrt{2}}\left(\xi_{11}(t)\xi_{20}(t)-\xi_{10}(t)\xi_{21}(t)\right)\\\frac{1}{6}\left(\sqrt{2}\xi_{10}(t)^2-9\sqrt{2}\xi_{11}(t)\xi_{10}(t)-\sqrt{2}\xi_{20}(t)^2+9\sqrt{2}\xi_{20}(t)\xi_{21}(t)\right)\end{pmatrix}$$

Secular terms are equated to zero give certain solvability conditions and at this order,

$$\begin{aligned}
&a_0\left(14\sqrt{2}\left(135\alpha_0^2+16\Omega_2\right)-486\alpha_0 b_0\right)+224\sqrt{2}\alpha_0\Omega_2+9b_0\left(117\alpha_0^2-64\Omega_2\right)=0\\
&6\sqrt{2}a_0\left(585\alpha_0^2+64\Omega_2\right)+270\sqrt{2}\alpha_0 a_0^2+448\sqrt{2}\alpha_0\Omega_2+84b_0\left(27\alpha_0^2-16\Omega_2\right)\\
&-243\sqrt{2}\alpha_0 b_0^2=0\\
&2\sqrt{2}a_0\left(1755\alpha_0^2+224\Omega_2\right)-270\sqrt{2}\alpha_0 a_0^2+384\sqrt{2}\alpha_0\Omega_2+84b_0\left(27\alpha_0^2-16\Omega_2\right)\\
&+243\sqrt{2}\alpha_0 b_0^2=0\\
&2a_0\left(7\sqrt{2}\left(135\alpha_0^2+16\Omega_2\right)+243\alpha_0 b_0\right)+224\sqrt{2}\alpha_0\Omega_2+3b_0\left(351\alpha_0^2-224\Omega_2\right)=0,
\end{aligned}\tag{5.7}$$

and there are three solutions to these conditions, namely

$$\omega_2=-\frac{135}{32}\left(\sqrt{2}\alpha_0^2+2\alpha_0^2\right),a_0=-\sqrt{2}\alpha_0-\alpha_0,b_0=0\tag{5.8}$$

$$\omega_2 = -\frac{135}{32}\left(\sqrt{2}\alpha_0^2 + 2\alpha_0^2\right), a_0 = +\sqrt{2}\alpha_0 - \alpha_0, b_0 = 0 \tag{5.9}$$

and

$$\omega_2 = 0, a_0 = 0, b_0 = 0. \tag{5.10}$$

The first two solutions for the constants in Equations (5.8) and (5.9) each represent a family of periodic orbits with different frequencies and different a_0. The third solution, Equation (5.10) leads to the trivial solution for ξ_{13}, ξ_{23}, η_{13}, and η_{23}, seen by carrying out the expansion to $O(\delta^3)$.

Solutions at second order corresponding to $\mathbf{x}_2$ with the solvability condition as in Equation (5.8) applied are

$$\begin{aligned}
\xi_{12} &= \frac{1}{384}\left(-1296\sqrt{2}\alpha_0^3 - 2592\alpha_0^3 - 192\sqrt{2}\alpha_0^2 - 192\alpha_0^2\right) \\
&+ \frac{1}{384}\left(783\sqrt{2}\alpha_0^3 + 1566\alpha_0^3 + 128\sqrt{2}\alpha_0^2 + 128\alpha_0^2\right)\cos(t) \\
&+ \frac{1}{384}\left(432\sqrt{2}\alpha_0^3 + 864\alpha_0^3 + 64\sqrt{2}\alpha_0^2 + 64\alpha_0^2\right)\cos(2t) \\
&+ \frac{1}{384}\left(81\sqrt{2}\alpha_0^3 + 162\alpha_0^3\right)\cos(3t) \\
\xi_{22} &= \frac{1}{384}\left(3888\sqrt{2}\alpha_0^3 + 5184\alpha_0^3 - 192\sqrt{2}\alpha_0^2 - 192\alpha_0^2\right) \\
&+ \frac{1}{384}\left(-2349\sqrt{2}\alpha_0^3 - 3132\alpha_0^3 + 128\sqrt{2}\alpha_0^2 + 128\alpha_0^2\right)\cos(t) \\
&+ \frac{1}{384}\left(-1296\sqrt{2}\alpha_0^3 - 1728\alpha_0^3 + 64\sqrt{2}\alpha_0^2 + 64\alpha_0^2\right)\cos(2t) \\
&+ \frac{1}{384}\left(-243\sqrt{2}\alpha_0^3 - 324\alpha_0^3\right)\cos(3t) \\
\eta_{12} &= \frac{1}{576}\left(837\sqrt{2}\alpha_0^3 + 837\alpha_0^3 - 64\sqrt{2}\alpha_0^2 - 128\alpha_0^2\right)\sin(t) \\
&+ \frac{1}{576}\left(-864\sqrt{2}\alpha_0^3 - 864\alpha_0^3 - 64\sqrt{2}\alpha_0^2 - 128\alpha_0^2\right)\sin(2t) \\
&+ \frac{1}{576}\left(-243\sqrt{2}\alpha_0^3 - 243\alpha_0^3\right)\sin(3t) \\
\eta_{22} &= \frac{1}{576}\left(-1674\sqrt{2}\alpha_0^3 - 2511\alpha_0^3 - 64\sqrt{2}\alpha_0^2 - 128\alpha_0^2\right)\sin(t) \\
&+ \frac{1}{576}\left(1728\sqrt{2}\alpha_0^3 + 2592\alpha_0^3 - 64\sqrt{2}\alpha_0^2 - 128\alpha_0^2\right)\sin(2t) \\
&+ \frac{1}{576}\left(486\sqrt{2}\alpha_0^3 + 729\alpha_0^3\right)\sin(3t)
\end{aligned} \tag{5.11}$$

The Lyapunov center theorem does not hold in this case because there is a resonant frequency for all values of δ. Nonetheless, when the eigenvalues are imaginary, there are still two (and maybe even three) distinct families of periodic

orbits that branch out from the constant solution. To the order we need for perturbation theory, the Hamiltonian is of the form

$$H = \omega/2(\eta_1^2 + \eta_2^2) + V(\xi_1, \xi_2, \epsilon).$$

That is, the energy can be split into kinetic and potential in the standard way.

CHAPTER 6

POSSIBLE EXTENSIONS

Johansson shows numerically, that for N just above the first HH bifurcation, small perturbations of the nodal solution remain small, while for somewhat larger values of N small perturbations grow, and their images make large excursions around phase space [19]. Through numerically-calculated Poincaré maps, he shows that these orbits are chaotic. This is the "new type of self-trapping transition" referred to by the title of this paper. While "chaos" itself is hard to define, in fact there is no one accepted definition, it is usually described as having characteristics of sensitivity to initial conditions and a dense collection of points with peiodic orbits. We have a conjecture for why this chaos occurs and have begun writing the numerical software that would demonstrate it.

The nonempty intersection of the stable and unstable manifolds of a point x_0, denoted as $W_s(x_0)$ and $W_u(x_0)$ respectively, is called a homoclinic orbit. If one iterates the map forward a number of times, the point gets closer and closer to the equilibrium point since it lies on the stable manifold. However, the point also lies on the unstable manifold. Therefore, the existence of one homoclinic point implies that there is an infinite number of them and this property gives rise to the chaos seen by Johansson. Transverse heteroclinic and/or homoclinic orbits might exist between the different forms of the nodal solution. In addition to the nodal solution (3.4) mentioned earlier in this dissertation, there are two more solutions with the same structure but with the

three elements permuted, allowing the zero to be found in either of the other vector components:

$$\mathbf{\Psi}_z = \sqrt{\frac{N}{2}} \begin{pmatrix} 1 \\ 0 \\ -1 \end{pmatrix} e^{i\left(3-\frac{N}{2}\right)t}, \qquad \mathbf{\Psi}_z = \sqrt{\frac{N}{2}} \begin{pmatrix} 0 \\ 1 \\ -1 \end{pmatrix} e^{i\left(3-\frac{N}{2}\right)t}, \qquad \mathbf{\Psi}_z = \sqrt{\frac{N}{2}} \begin{pmatrix} 1 \\ -1 \\ 0 \end{pmatrix} e^{i\left(3-\frac{N}{2}\right)t}.$$

This is simply because the equations of motion are invariant to permutations of the elements.

When $N - N_{H1} > 0$ but small, all three of these solutions are unstable. Each will have a stable and unstable manifold, but these manifolds should be localized in a neighborhood of each of the standing waves, trapping small perturbations in a neighborhood of the standing wave. As N is increased, these manifolds which start out as closed loops should grow, and for N sufficiently large the unstable manifold of one solution will intersect the stable manifolds of each of the other two, or vice versa, resulting in a large-scale heteroclinic tangle. This should give a mechanism by which small initial perturbations may take large excursions. The stable manifolds cannot intersect with each other (similarly for unstable manifolds) because of the differentiability of any vector field, in this case of the Poincaré map.

One could investigate the phase space through the use of numerics. By numerically computing stable and unstable manifolds of the Poincaré map, the points at which the manifolds of one nodal solution intersect with the manifolds of the other nodal solutions can be found, resulting in the homoclinic orbits mentioned above. This can be difficult, however since the Poincaré map cannot be defined analytically.

CHAPTER 7

CONCLUSION

The many solutions, bifurcations, instabilities, and chaos associated with the system of ODEs related to the NLS are identified and explained. These dynamics can be especially useful in explaining the behavior of many physical phenomena including water waves, semiconductors, Bose-Einstein condensates in an open lattice, and also nonlinear optics and wave guide arrays. The periodic solutions and their behavior may be useful to encode data.

A discretized version of the focusing NLS with three wells and periodic boundary conditions was studied. We used the properties of Hamiltonian systems, perturbation theory, normal forms, and linearization to understand the dynamics of the DNLS, and are interested in the two standing wave solutions that undergo a Hamiltonian-Hopf bifurcation and a symmetric transcritical bifurcation.

The waveguides in our problem are arranged in a triangle. The stable solutions in the DNLS correspond to a steady light brightness in the waveguides, and periodic solutions correspond to periodic jumping between the light observed within the three waveguides. Moreover, chaos represents that the light is randomly jumping from one waveguide to another.

We began with diagonalization, then reduced the number of the degrees of freedom from three down to two using Nöther's Theorem (since the system has rotational symmetry). The standing wave solutions can be found analytically. For

the Hamiltonian Hopf bifurcation and its two types, we used a canonical change of variables, one that preserves Hamilton's equations. This change comes from the Burgoyne-Cushman algorithm which is used to calculate normal forms of real linear Hamiltonians with purely imaginary eigenvalues. A projection technique was used to discover resonant terms of the normal form Hamiltonian. These resonant terms determine the type of Hamiltonian Hopf bifurcation that surrounds the parameter N at particular critical values. Additional analysis was performed on the solution which undergoes the HH bifurcation, namely the nodal solution. We reduce the system again through a polar canonical change of variables in order to plot Poincaré maps and phase planes for this solution with different parameter values.

For the constant solution which undergoes a transcritical bifurcation, a different reduction of the degrees of freedom was computed, though using the same techniques. In addition, the same projection technique mentioned above was used for this solution to obtain the resonant terms of this normal form Hamiltonian. We then used Lie transforms and Poincaré Lindstedt expansion to find periodic orbits of the constant solution.

The methods discussed in this dissertation are powerful tools for understanding the behavior of the standing wave solutions to the three-mode DNLS in the nonlinear regime for small amplitudes with periodic boundary conditions. In particular, calculating normal forms helps to determine the important terms in an equation, and in a sense "simplifies away" others. Though higher order terms are introduced, those terms can be further split up into resonant and nonresonant parts using projection techniques.

Johansson studied the Hamiltonian Hopf bifurcation numerically, discussing what happens for each of the two types near the critical parameter values $N = 9.077$ and $N = 18$. We provide more analytical insight into the dynamics of the standing wave solution associated with this HH bifurcation and that of the symmetric transcritical bifurcation associated with the constant solution as well.

The DNLS is a widely studied equation. While many others have found standing wave solutions to the DNLS and have studied Hamiltonian systems, we have described the phase space of these solutions and make a statement on the dynamics. When considered as a model of nonlinear optics, the DNLS describes the evolution of a wave traveling inside of a nonlinear waveguide. We believe that in an experimental setting, the dynamics of these standing wave solutions that have been discovered in this dissertation could be tested and confirmed.

APPENDIX A

THE BURGOYNE-CUSHMAN ALGORITHM

The Burgoyne Algorithm takes as input a Hamiltonian matrix A with purely imaginary eigenvalues of multiplicity greater than one, and returns a change of variables that puts that matrix in a canonical form that is something like a Jordan normal form.

The algorithm returns the normal form

$$B = \left(\begin{array}{cc|cc} 0 & \Omega & 0 & 0 \\ -\Omega & 0 & 0 & 0 \\ \hline -\sigma & 0 & 0 & \Omega \\ 0 & -\sigma & -\Omega & 0 \end{array}\right). \tag{A.1}$$

We use it to obtain the canonical change of variables for the quadratic part of the reduced Hamiltonian H_2 in equation (3.15) at $N = 18$ where the second HH bifurcation occurs. The same can be done at $N = 9.077$ where the other HH bifurcation occurs, but we are forced to use numerical values instead of exact symbolic arithmetic.

This algorithm computes a symplectic change of variables P such that $A = P^{-1}BP$ with $A = JH$, where H is symmetric. The characteristic polynomial is assumed to be of the form $p(\lambda) = (\lambda^2 + \alpha^2)^n$ where A is a $2n$ by $2n$ matrix as above

and $\alpha > 0$. Before the algorithm can be used, one must decompose A into semisimple and nilpotent parts, Σ and N respectively. Burgoyne points out that

$$\Sigma = A\left\{1 + \sum_{j=1}^{m-1} \binom{2j}{j} \left(\frac{p(A)}{4\alpha^2}\right)^j\right\}$$

and $N = A - \Sigma$ where m is chosen so that $p(A)^m = 0$ but $p(A)^{m-1} \neq 0$ and clearly $m \leq n$. The algorithm is recursive, so suppose the sets $W_0 = \{0\}$ through W_{j-1} for $j = 1$ have already been found. Define K_i for $1 \leq i \leq m$ to be the set of all vectors $\mathbf{x} \in \mathbb{R}^{2n}$ such that $N^i\mathbf{x} = 0$ and $K_0 = \{0\}$. Note that $K_m = \mathbb{R}^{2n}$. Next define the inner product $\langle \mathbf{x}, \mathbf{y} \rangle = \mathbf{x}J^\top\mathbf{y}$ $\forall \mathbf{x}, \mathbf{y} \in \mathbb{R}^{2n}$. $W_{j=1}^\perp$ is the set of all vectors $x \in \mathbb{R}^{2n}$ such that $\langle \mathbf{x}, \mathbf{w} \rangle = 0$ for all $\mathbf{w} \in W_{j-1}$. Next, we must find $t = t_j$ such that $0 \leq t \leq m$ and

$$W_{j-1}^\perp \cap K_{t+1} = W_{j-1}^\perp$$

but

$$W_{j-1}^\perp \cap K_t \neq W_{j-1}^\perp.$$

Note that if $N = 0$, (i.e., $m = 1$), then $t = 0$.

For the Hamiltonian of the general form (2.9) defined at N_{H2}, and similarly at N_{H1}, $m = 2$, $j = 1, 2$, $i = 1, 2$ $n = 2$ and we find that the sets are $W_0 = \{0\}$ and

$W_0^{\perp} = \{\mathbb{R}^4\}$. $K_0 = \{0\}$ and $K_1 = \{\mathbf{x} = (x_1, x_2, y_1, y_2) | N\mathbf{x} = 0\}$ where

$$N = \begin{pmatrix} 0 & 0 & \frac{3}{4} & -\frac{3}{2\sqrt{2}} \\ 0 & 0 & -\frac{3}{2\sqrt{2}} & \frac{3}{2} \\ -\frac{3}{4} & -\frac{3}{4\sqrt{2}} & 0 & 0 \\ -\frac{3}{4\sqrt{2}} & -\frac{3}{8} & 0 & 0 \end{pmatrix}$$

and $K_2 = \mathbb{R}^4$ since $N^2 = 0$. In this case $t = 1$, but in general the algorithm is defined slightly differently depending on whether t is even or odd.

Since $t = 1$ is odd, the first step is to choose $\mathbf{z} \in W_{j-1}^{\perp}$ such that $\mathbf{z} \notin K_t$ and $\langle \mathbf{z}, N^t \mathbf{z} \rangle = \epsilon_j$ where $\epsilon_j^2 = 1$. For the matrix under consideration, $\mathbf{z} \notin K_1$ but $\langle \mathbf{z}, N\mathbf{z} \rangle = \pm 1$.

Let $\mathbf{z}_j$ be the space spanned by vectors of the form $N^k z$ and $N^k \Sigma z$, $N^k \Sigma \mathbf{z}$ for $0 \leq k \leq t$ and put $W_j = \mathbf{z}_j + W_{j-1}$. If $W_j \neq \mathbb{R}^{2n}$ repeat until $W_l = \mathbb{R}^{2n}$ for some l.

We have the choice of $\mathbf{z}$ to form z_i for $1 \leq i \leq r$.

$r = \frac{1}{2}(i+1) = 1$ so we need only z_0 and z_1. Define

$$z_i = z_{i-1} + \frac{\epsilon}{2\alpha^2} \langle z_{i-1}, \Sigma N^{t+1-2i} z_{i-1} \rangle N^{2i-1} \Sigma z_{i-1}$$

$z_0 = z$ and $\widetilde{z_0} = z_1$. $t = r = 1$.

Now,

$$\tau = \tau_j = \begin{cases} 0 & j = 1 \\ \sum_{i=1}^{j-1} (t_i + 1) & j \neq 1 \end{cases}$$

So $\tau_1 = 0$ and $z_* = \widetilde{z}_{r-1} = \widetilde{z}_0 = z_1$. Finally, the basis for z_j is $b_1 = z_*$, $b_2 = \frac{1}{\alpha}\Sigma z_*$, $b_3 = \epsilon N^t z_* = \epsilon N z_*$, and $b_4 = \frac{\epsilon}{\alpha}\Sigma N^t z_* = \frac{\epsilon}{\alpha}\Sigma N z_*$. This provides the matrix $P = \{b_1, b_2, b_3, b_4\}^\top$ defining the needed change of variables.

For $N = 9.077$, the Burgoyne-Cushman calculates P as

$$P = \begin{pmatrix} 0.7423 & 0.9010 & -0.4874 & -0.7114 \\ -0.2195 & 0.9835 & -0.2862 & -0.4177 \\ -0.2195 & 1.4543 & 0.6097 & -0.4177 \\ 1.4810 & -0.8473 & -1.0383 & 0.7114 \end{pmatrix}, \tag{A.2}$$

and for $N = 18$,

$$P = \begin{pmatrix} \frac{1}{\sqrt{3}} & 0 & 0 & 0 \\ \frac{5}{6\sqrt{6}} & \frac{1}{3} & 0 & 1 \\ \frac{1}{\sqrt{3}} & \frac{5}{6\sqrt{2}} & \sqrt{3} & 0 \\ 0 & -1 & 0 & 0 \end{pmatrix}. \tag{A.3}$$

BIBLIOGRAPHY

[1] V. Arnol'd, editor. *Dynamical Systems III*, volume 3. Springer-Verlag Berlin Heidelberg, 1988.

[2] P. Buonsante, R. Franzosi, and V. Penna. Dynamical instability in a trimeric chain of interacting Bose-Einstein condensates. *Physical Review Letters*, 90:050404, 2003.

[3] N. Burgoyne and R. Cushman. Normal forms for real linear Hamiltonian systems with purely imaginary eigenvalues. *Celestial mechanics*, 8(4):435–443, 1974.

[4] G. M. Chechin and V. P. Sakhnenko. Interactions between normal modes in nonlinear dynamical systems with discrete symmetry. exact results. *Physica D*, 117(1-4):43–76, 1998.

[5] S-N Chow and Y-I Kim. Bifurcation of periodic orbits for non-positive definite Hamiltonian systems. *Applicable Analysis*, 31:163–199, 1988.

[6] S. Defilippo, M. F. Girard, and M. Salerno. Lyapunov exponents for the N=3 discrete self-trapping equation. *Physica D*, 26(411):254, 1987.

[7] J. C. Eilbeck and M. Johansson. The discrete nonlinear Schrödinger equation – 20 years on. In L. Vázquez, R. S. MacKay, and M. P. Zarzano, editors, *Proceedings of the third conference on localization and energy transfer in nonlinear systems*, pages 44–67. World Scientific, 2003.

[8] J. C. Eilbeck, P. S. Lomdahl, and A. C. Scott. The discrete self trapping equation. *Physica D*, 16(318), 1985.

[9] N. Finlayson and G. I. Stegeman. Spatial switching, instabilities, and chaos in a three waveguide nonlinear directional coupler. *Appl. Phys. Lett.*, 56:2276, 1990.

[10] L. Y. Glebsky and L. M. Lerman. On small stationary localized solutions for the generalized Swift-Hohenberg equation. *Chaos*, 5:424, 1994.

[11] M. Golubitsky and I. Stewart. *The Symmetry Perspective: From Equilibrium to Chaos in Phase Space and Physical Space*. Progress in Mathematics. Birkhäuser Basel, 2003.

[12] R. H. Goodman. Hamiltonian-Hopf bifurcations and dynamics of NLS/GP standing wave modes. *Journal of Physics A: Mathematical and General*, 44(42):425101, 2011.

[13] R. H. Goodman and M. I. Weinstein. Stability and instability of nonlinear defect states in the coupled mode equations- analytical and numerical study. *Physica D*, 237:2731–2760, 2008.

[14] D. Hennig. The discrete self-trapping equation and the Painleve property. *Journal of Physics A: Mathematical and General*, 25(5):1247, 1992.

[15] D. Hennig. Existence of nonlinear normal modes for coupled nonlinear oscillators. *Nonlinear Dynamics*, 80(1):937–944, 2015.

[16] D. Hennig, J. Dorignac, and D. K. Campbell. Transfer of Bose-Einstein condensates through discrete breathers in an optical lattice. *Physical Review A*, 82:053604, 2010.

[17] D. Hennig and H. Gabriel. The four-element discrete nonlinear Schrödinger equation-non-integrability and Arnold diffusion. *Journal of Physics A: Mathematical and General*, 28(13):3749, 1995.

[18] D. Hennig, H. Gabriel, M. F. Jorgensen, P. L. Christiansen, and C. B. Clausen. Homoclinic chaos in the discrete self-trapping trimer. *Phys. Rev. E*, 51:2870–2876, 1995.

[19] M. Johansson. Hamiltonian Hopf bifurcations in the discrete nonlinear Schr´odinger trimer: oscillatory instabilities, quasi-periodic solutions and a 'new' type of self-trapping transition. *Journal of Physics A: Mathematical and General*, 37(6):2201, 2004.

[20] T. Kapitula, P. G. Kevrekidis, and Z. Chen. Three is a crowd: Solitary waves in photorefractive media with three potential wells. *SIAM Journal on Applied Dynamical Systems*, 5(4):598–633, 2006.

[21] T. Kapitula, P. G. Kevrekidis, and D. Yan. The Krein matrix: General theory and concrete applications in atomic Bose-Einstein condensates. *SIAM Journal of Applied Mathematics*, 73:1368–1395, 2013.

[22] E. W. Kirr, P. G. Kevrekidis, E. Shlizerman, and M. I. Weinstein. Symmetry-breaking bifurcation in nonlinear Schrödinger/Gross-Ptaevskii equations. *SIAM Journal on Mathematical Analysis*, 40:566–604, 2008.

[23] A. Lahiri and M. S. Roy. The Hamiltonian Hopf bifurcation: an elementary perturbative approach. *International Journal of Non-Linear Mechanics*, 36:782–802, 2001.

[24] K. Law and E. Hoq. The dynamics of unstable waves. In P. G. Kevrekidis, editor, *The Discrete Nonlinear Schrödinger Equation*, volume 232 of *Springer Tracts in Modern Physics*, pages 215–228. Springer, 2009.

[25] P. Liberman and C.-M. Marle. *Symplectic geometry and analytical mechanics*, volume 35. Springer Netherlands, 1987.

[26] R. S. MacKay. Stability of equibrium of Hamiltonian systems. *Nonlinear Phenomena and Chaos*, pages 254–270, 1986.

[27] K. R. Meyer and G. R. Hall. *Introduction to Hamiltonian dynamical systems and the N-body problem*. Applied Mathematical Sciences. Springer-Verlag, New York, 1992.

[28] K. R. Meyer and D. S. Schmidt. Periodic orbits near L4 for mass ratios near the critical mass ratio of Routh. *Celestial Mechanics*, 4:99–109, 1971.

[29] M. I. Molina, W. D. Deering, and G. P. Tsironis. Applications of self-trapping in optically coupled devices. *Physica D*, 68:135–137, 1993.

[30] M. I. Molina, W. D. Deering, and G. P. Tsironis. Optical switching in 3-coupler configurations. *Physica D*, 66:135–142, 1993.

[31] M. I. Molina and G. P. Tsironis. Tuning the Kenkre-Campbell self-trapping transition. *Physical Review A*, 46:1124–1127, 1992.

[32] J. A. Montaldi, R. M. Roberts, and I. N. Stewart. Periodic solutions near equilibria of symmetric Hamiltonian systems. *Philosophical Transactions of the Royal Society of London. Series A, Mathematical and Physical Sciences*, 325(1584):237–293, 1988.

[33] P. Panayotaros. Instabilities of breathers in a finite NLS lattice. *Physica D*, 241(8):847–856, 2012.

[34] A. Sacchetti. Nonlinear Schrödinger equations with multiple-well potential. *Physica D: Nonlinear Phenomena*, 241:1815–1824, 2012.

[35] H. Susanto. Few-lattice-site systems of discrete self-trapping equations. In P. G. Kevrekidis, editor, *The Discrete Nonlinear Schrödinger Equation*, volume 232 of *Springer Tracts in Modern Physics*, pages 249–257. Springer, 2009.